Effects of spatially heterogeneous lakeside development on nearshore biotic communities in a large, deep, oligotrophic lake (Lake Baikal, Siberia)

Michael F. Meyer[1]*

Ted Ozersky[2]

Kara H. Woo[3]

Kirill Shchapov[2]

Aaron W. E. Galloway[4]

Julie B. Schram[4]

Emma J. Rosi[5]

Daniel D. Snow[6]

Maxim A. Timofeyev[7]

Dmitry Yu. Karnaukhov[7]

Matthew R. Brousil[3]

Stephanie E. Hampton[3]

[1.] School of the Environment, Washington State University, Pullman, WA, USA

[2.] Large Lakes Observatory, University of Minnesota - Duluth, Duluth, MN, USA

[3.] Center for Environmental Research, Education, and Outreach, Washington State University, Pullman, WA, USA

[4.] Oregon Institute of Marine Biology, University of Oregon, Charleston, OR, USA

[5.] Cary Institute of Ecosystem Studies, Millbrook, NY, USA

[6.] School of Natural Resources, University of Nebraska-Lincoln, Lincoln, NE, USA

[7.] Biological Research Institute, Irkutsk State University, Irkutsk, Irkutsk Oblast, Russia

*corresponding author: michael.f.meyer@wsu.edu

Keywords: sewage, PPCP, food webs, fatty acids, human disturbance

Statement of novelty, significance, and breadth of interest of the science presented in the proposed manuscript

We examined food web consequences of spatially heterogeneous disturbance associated with small human settlements along the shoreline of remote oligotrophic Lake Baikal, illustrating that nuanced biotic effects can occur at low levels of nutrient pollution. Using sewage-specific indicators (pharmaceuticals and personal care products - PPCPs), we demonstrated that increased nutrients at three discrete lakeside developments (80-1,963 permanent residents) and the associated increased filamentous benthic algal abundance were consistent with sewage pollution. This is the first study to provide such robust evidence that recent benthic algal blooms are caused by sewage. These changes in benthic algae altered resources and nutrition for grazing invertebrates, and macroinvertebrate composition accordingly differed at disturbed sites. Stable isotope and fatty acid analysis of benthic algae and macroinvertebrates suggested that grazers at sewage disturbed sites compensate for changing resource nutrition through behavior or altered metabolism. This study demonstrates how patchy, low-level eutrophication of oligotrophic systems can cause food webs to respond in less visible ways. Further, Baikal is an iconic ancient lake, holding 20% of the world's fresh surface water and harboring the highest endemism and biodiversity known in a lake; thus, understanding human impacts on this system is of both societal importance and broad scientific interest.

Statement indicating why L&O is the best outlet for the work

This manuscript will appeal to L&O readers who are interested in both basic and applied issues. From a basic ecology perspective, we investigate how bottom-up disturbances along a gradient can propagate throughout a food web. From an applied perspective, we highlight how our results

50 can inform monitoring programs, especially as long-term littoral monitoring tends to be
51 uncommon relative to pelagic efforts. In addition, we use a suite of techniques that crosses
52 subdisciplines in a manner appreciated by limnologists and oceanographers, and less familiar to
53 other disciplines, such that L&O seems like the perfect home for this manuscript.
54
55 **Abstract**
56 Sewage released from lakeside development can reshape ecological communities. In particular,
57 nearshore periphyton can rapidly assimilate sewage-associated nutrients, leading to increases of
58 filamentous algal abundance, thus altering both food abundance and quality for grazers. In Lake
59 Baikal, a large, ultra-oligotrophic, remote lake in Siberia, filamentous algal abundance has
60 increased near lakeside developments, and localized sewage input is the suspected cause. These
61 shifts are of particular interest in Lake Baikal, where endemic littoral biodiversity is high,
62 lakeside settlements are mostly small, tourism is relatively high (~1.2 million visitors annually),
63 and settlements are separated by large tracts of undisturbed shoreline, enabling investigation of
64 heterogeneity and gradients of disturbance. We surveyed sites along 40 km of Baikal's
65 southwestern shore for sewage indicators – pharmaceuticals and personal care products (PPCPs)
66 and microplastics – as well as periphyton and macroinvertebrate abundance and indicators of
67 food web structure (stable isotopes and fatty acids). PPCPs, including caffeine and
68 acetaminophen/paracetamol, were spatially related to lakeside development. As predicted,
69 lakeside development was associated with more filamentous algae and lower abundance of
70 sewage-sensitive mollusks. Periphyton and macroinvertebrate stable isotopes and essential fatty
71 acids suggested that food web structure otherwise remained similar across sites; yet, the
72 invariance of amphipod fatty acid composition, relative to periphyton, suggested that grazers

adjust behavior or metabolism to compensate for different periphyton assemblages. Our results demonstrate that even low levels of human disturbance can result in spatial heterogeneity of nearshore ecological responses, with potential for creating less visible effects that propagate through the food web.

Introduction

The release of treated and untreated wastewater into aquatic ecosystems is a common human disturbance that can introduce pollutants and reshape aquatic ecological communities (Moore et al. 2003). Nitrogen and phosphorus are among the primary pollutants in wastewater and its associated byproducts (Smith et al. 1999), yet these nutrients can also originate from disparate anthropogenic and natural environmental sources, thereby complicating their use as sewage indicators. For example, agriculture (Powers et al. 2016), watershed processes such as melting permafrost (Turetsky et al. 2000), and changes in terrestrial plant communities (Moran et al. 2012) can all increase allochthonous nutrient inputs similar to sewage. Regardless of the nutrients' source, biological processes can further confound sewage detection. Benthic primary producers, especially those in oligotrophic systems, can assimilate nutrients quickly from the water column (e.g., hours), such that elevated nutrient concentrations may not be not observed (Hadwen and Bunn 2005).

Because nutrients come from numerous non-sewage sources, indicators consistently associated with human activity, such as enhanced $\delta^{15}N$ stable isotope signatures (Costanzo et al. 2001; Camilleri and Ozersky 2019), pharmaceuticals and personal care products (PPCPs) (Rosi-Marshall and Royer 2012; Meyer et al. 2019) and microplastics (Barnes et al. 2009), have garnered increasing attention for their usefulness as sewage indicators. Stable isotopes, such as

97 $\delta^{15}N$, have been frequently used to trace sewage pollution (Gartner et al. 2002), yet their
98 potential to indicate sewage can be obfuscated by complex terrestrial (Craine et al. 2018) and
99 aquatic (Guzzo et al. 2011) processes. PPCP studies from continental (Kolpin et al. 2002;
100 Focazio et al. 2008; Yang et al. 2018) to colloidal pore (Yang et al. 2016) scales, have shown
101 that PPCP concentrations tend to be greatest closer to their source. In addition to identifying
102 areas and periods of sewage pollution, PPCPs have also demonstrated robustness in defining
103 gradients of sewage pollution in river systems, with concentrations being directly proportional to
104 population density and inversely proportional to distance from a densely populated area (Bendz
105 et al. 2005). Similar to PPCPs, microplastics (plastic debris up to 5 mm in size) also have been
106 useful to detect sewage pollution (Li et al. 2018) along gradients of increasing human population
107 density (Klein et al. 2015), although they can sometimes originate from non-sewage sources,
108 such as shoreline debris or fishing nets (Free et al. 2014). In contrast to $\delta^{15}N$ signatures and
109 PPCPs concentrations, microplastics are typically resistant to degradation (Barnes et al. 2009),
110 providing a signal over a longer time frame than many PPCPs and nutrients in sewage. As a
111 result of each pollutant's consistent association with sewage, co-located $\delta^{15}N$, PPCP, and
112 microplastic measurements can be used to infer the spatial extent and timing of sewage pollution
113 in an ecosystem.
114
115 The effects of sewage pollution are frequently first seen in nearshore benthic communities where
116 increased nutrients alter algal species composition, abundance, nutritional quality, as well as
117 food web trophic structure. Increased filamentous algal abundance, for example, has been
118 frequently observed in areas suspected of sewage pollution (Rosenberger et al. 2008; Hampton et
119 al. 2011), likely due to benthic filamentous algae efficiently removing nutrients from the water

column (Hadwen and Bunn 2005; Andersson and Brunberg 2006). With a changing resource base, grazing macroinvertebrate communities may likewise shift to include more detritivores or species capable of consuming filamentous algae (Rosenberger et al. 2008). In addition to some grazers' physical difficulty consuming filamentous algae (Mazzella and Russo 1989), there also may be changes in algal nutritional quality, as filamentous algae tend to contain a different mixture of essential fatty acids (EFAs) in comparison to diatoms (Kelly and Scheibling 2012), which dominate periphyton communities in unimpacted ecosystems. In particular, the EFAs 18:3ω3 and 18:2ω6 are commonly associated with green filamentous algae (Taipale et al. 2013), whereas 20:5ω3 is more associated with diatoms (Taipale et al. 2013). All EFAs are largely synthesized by primary producers, and each related group produces strongly differentiated multivariate signatures (Taipale et al. 2013; Galloway and Winder 2015). Consumers can acquire fatty acids by grazing (Dalsgaard et al. 2003) or upgrading fatty acids at their own energetic expense (Sargent and Falk-Petersen 1988; Dalsgaard et al. 2003) and often reflect the fatty acid signatures of their diets. Thus, comparing consumer and producer fatty acid compositions can be used to infer how grazing patterns change in response to increasing sewage pollution.

To investigate lake littoral community and food web responses to sewage pollution, we surveyed 40 km of Lake Baikal's shoreline for indicators of sewage pollution and metrics of benthic community composition and structure. Located in Siberia, Lake Baikal is the oldest, most voluminous, and deepest freshwater lake in the world (Hampton et al. 2018), with the majority of Lake Baikal's biodiversity occurring in the littoral zone (Kozhova and Izmest'eva 1998). While Lake Baikal's pelagic zone is generally ultra-oligotrophic (Yoshida et al. 2003; O'Donnell et al. 2017), nearshore areas abutting lakeside settlements have shown distinct signs of eutrophication

(Timoshkin et al. 2016). Much of Lake Baikal's shoreline lacks human development, and Baikal's watershed is largely roadless and unpopulated (Moore et al. 2009). Despite low levels of development, uncharacteristic filamentous algal blooms have been occurring throughout the lake since 2010 (Kravtsova et al. 2014; Timoshkin et al. 2016; Volkova et al. 2018). While increased *Ulothrix* spp. abundance historically occurs in late summer (Kozhov 1963; Kozhova and Izmest'eva 1998), recent observations of *Spirogyra* spp. abundance at unprecedented levels are thought to be associated with increased nearshore nutrient concentrations (Volkova et al. 2018; Ozersky et al. 2018). Inadequate wastewater management in lakeside settlements is likely the main driver of these nearshore algal blooms (Timoshkin et al. 2016, 2018), motivating further research to identify the extent to which sewage is altering nearshore communities

Given the growing evidence that Baikal's nearshore periphyton communities are responding to sewage inputs, our goal was to understand how littoral benthic community composition and interactions may be changing near areas of sewage pollution. This overarching goal was divided into three specific objectives:

1. identify areas of wastewater pollution using consistent sewage indicators,
2. assess the relationship between sewage indicators and littoral periphyton and macroinvertebrate community composition, and
3. evaluate how food webs may restructure with increasing sewage pollution.

We hypothesized that (1) sewage indicators, such as PPCP concentrations, $\delta^{15}N$, and microplastic densities, would increase with increasing population density and proximity of lakeside development; (2) an increasing sewage signal would correlate with increased dominance of filamentous benthic algae; and (3) increasing filamentous algae abundance would result in

changes in the abundance of different macroinvertebrate feeding guilds, reflected in community composition and dietary tracers such as carbon and nitrogen stable isotopes and fatty acids.

Methods

Site description

The vast majority of Lake Baikal's 2,100-km shoreline lacks lakeside development (Moore et al. 2009; Timoshkin et al. 2016). Our study focused on a 40-km section of Baikal's southwestern shoreline, which included three settlements of different sizes (Figure 1; Figure 2). From 19 through 23 August 2015, we sampled 14 littoral and 3 pelagic locations along our 40-km transect. Littoral locations were chosen to capture a range of sites with varying degrees of adjacent shoreline development – from "developed" (along the waterfront of human settlements) to "undeveloped" (no adjacent human settlements and complete forest cover; Figure 1; Figure 2; Table 1). Pelagic sites were located 2 to 5 km offshore from each of the developed sites in water depths of 900 to 1300 m (Figure 1; Table 1). All littoral sites were sampled at approximately the same depth (~1.25 m) at a distance of 8.90 to 20.75 m from shore (Table 1). At each site, air temperature was measured with a mercury thermometer, and photographs were taken of the substrate and the shoreline.

Three discrete lakeside settlements were located along our 40-km transect. The largest, Listvyanka, is primarily a tourist town of approximately 2000 permanent residents, although tourism can contribute significantly to the town's population with approximately 1.2 million annual visitors (Interfax-Tourism 2018). The other two settlements are the villages Bolshie Koty and Bolshoe Goloustnoe, which have approximately 80 and 600 permanent residents,

189 respectively. Bolshie Koty is home to two field research stations and several small tourist
190 accommodations. Bolshoe Goloustnoe has several hotels and tourist camps. Although Bolshie
191 Koty and Bolshoe Goloustnoe are built along small streams that empty into Baikal, there are no
192 upstream developed sites, meaning that any observed sewage indicators in Baikal most likely
193 originated either from Bolshie Koty or Bolshoe Goloustnoe.
194
195 *Inverse distance weighted (IDW) population calculation*
196 We recognized that sewage indicator concentrations at each sampling location may be related to
197 a sampling location's spatial position relative to both the size and proximity of neighboring
198 developed sites. Therefore, we created the inverse distance weighted (IDW) population metric to
199 compress, into a single metric, information about human population size, density, and location
200 along the shoreline as well as distance between developed sites and sampling locations. The
201 IDW metric reflects the idea that sewage pollution should be positively related to increasing
202 human density and inversely related with distance from densely populated areas (sensu Bendz et
203 al., 2005). Additionally, Timoshkin et al. (2018) noted that sewage enters Baikal's nearshore
204 largely through groundwater, implying that locations with more directly adjacent shoreline
205 development should experience higher sewage concentrations in the lake. Acknowledging that
206 nearshore PPCP concentrations were likely positively proportional to a developed location's
207 shoreline length, we scaled a developed site's population density by its shoreline length. This
208 scaling represents population density that directly interfaces with the lake, thereby capturing the
209 idea that sewage-associated pollutants, such as PPCPs (Karnjanapiboonwong et al. 2010) and
210 nutrients (de Vries 1972), contributed away from the shoreline can be removed via the soil
211 matrix en route to the lake.

Our calculation of IDW population was done in five steps. First, we traced polygons and shorelines from satellite imagery for each developed site in Google Earth. Polygons were traced for the entire area of visible development (Figure 2). Similarly, shoreline traces only reflected shoreline length for which there was visible development (Figure 2). Second, polygon and line geometries were downloaded from Google Earth as a .kml file. Third, the .kml file was imported into the R statistical environment (R Core Team 2019) where, using the sf package (Pebesma, 2018), we calculated shoreline length, polygon area, and centroid location for each developed site. Fourth, we joined point locations of each sampling site with the spatial polygons to calculate the distance from each sampling location to each developed site's centroid. Fifth, we calculated IDW population for each sampling location, using formula (1)

$$(1)\quad Ij = \frac{\frac{P_{LI}}{A_{LI}} * L_{LI}}{D_{j,LI}} + \frac{\frac{P_{BK}}{A_{BK}} * L_{BK}}{D_{j,BK}} + \frac{\frac{P_{BGO}}{A_{BGO}} * L_{BGO}}{D_{j,BGO}}$$

where I is the IDW population at sampling location j, P is the population at each of the three developed sites Listvyanka (LI), Bolshie Koty (BK), Bolshoe Goloustnoe (BGO), A is the area of a developed site in km^2, L is the shoreline length at a developed site in km, and D is the distance from sampling site j to each developed site's centroid in km. This formulation implies that all sampling locations are influenced by all three developed sites. Thus, the influence of an individual developed site on each sampling location is positively influenced by the size and spatial density of the population and its orientation toward the shoreline, and inversely proportional to a sampling location's distance from each of the three developed sites.

Water samples

At both pelagic and littoral sites, water samples were collected for nutrient, chlorophyll, microplastic, and PPCP analysis. Samples were collected by hand from 0.75 m depth for each littoral site and with a bucket from aboard the Irkutsk State University "Kozhov" research vessel for pelagic sites. Each water sample collection procedure is described below.

Nutrients

Water samples for nutrient analyses were collected in 150 mL glass jars that had been washed with phosphate-free soap and rinsed three times with water from the sampling location. Samples were collected in duplicates and immediately frozen at -20°C until processing at the A.P. Vinogradov Institute of Geochemistry (Siberian Branch of the Russian Academy of Sciences, Irkutsk). Samples were not filtered prior to freezing, meaning that nitrogen and ammonium concentrations may potentially include intracellular nitrogen and overestimate nitrogenous forms in the water column.

For each water sample, nitrate, ammonium, and total phosphorus concentrations were measured. For ammonium (2016a) and nitrate (2017) concentrations, samples were analyzed with a spectrophotometer following the addition of Nessler's reagent and disulfuric acid respectively. Total phosphorus concentration was measured with a spectrophotometer following the addition of persulfate (2016b). Concentrations are reported in mg/L.

Chlorophyll a

Water samples were collected in 1.5 L plastic bottles from a depth of approximately 0.75 m. Within 12 h of collection, three subsamples (up to 150 mL each) were filtered through 25-mm

diameter, 0.2 µm pore size nitrocellulose filters. Filters were then placed in a 35-mm petri dish and frozen in the dark until processing.

Chlorophyll samples were processed in a manner similar to that of Parsons and Strickland (1963) and Lorenzen (1967). Nitrocellulose filters were ground in 90% acetone, in which chlorophyll extraction was allowed to proceed overnight. Samples were then centrifuged for 15-20 minutes. After centrifugation, absorbance of the chlorophyll extract was measured in a spectrophotometer at 630, 645, 665, and 750 nm. Concentrations were calculated using the formula: $C = 11.64(A_{665} - A_{750}) - 2.16(A_{645} - A_{750}) - 0.1(A_{630} - A_{750}) / (V_2/V_1)$; where A is the absorbance value of a particular wavelength, V_1 is the volume of the filtered water, and V_2 is the volume of extract. Concentrations are reported as mg/L.

PPCPs

Water samples for PPCP analysis were collected in 250 mL amber glass bottles that were rinsed with either methanol or acetone and then three times with sample water prior to collections. Following collection, samples were refrigerated and kept in the dark until solid phase extraction (SPE).

Within 12 h of collection, samples were filtered directly from the amber glass bottle using an in-line Teflon filter holder with glass microfiber GMF (1.0 µm pore size, WhatmanGrad 934-AH) in tandem with a solid phase extraction (SPE) cartridge (200 mg HLB, Waters Corporation, Milford, MA) connected to a 1-liter vacuum flask. Lab personnel wore gloves and face masks to minimize contamination. Prior to filtration, SPE cartridges were primed with at least 5 mL of

either methanol or acetone and then washed with at least 5 mL of sample water. Rate of extraction was maintained at approximately 1 drop per second. Extraction proceeded until water could no longer pass through the SPE cartridge or until all collected water was filtered. Cartridges were stored in Whirlpacks at -20°C until analysis for 18 PPCP residues using liquid chromatography tandem mass spectrometry (LC-MS-MS) following methods of Lee et al. (2016) and D'Alessio et al (2018). Concentrations are reported in µg/L.

Microplastics

At each location, samples were collected in triplicate using 1.5 L clear plastic bottles that were washed thoroughly with sample water before each collection. Samples were collected by hand for each littoral site and with a metal bucket from aboard the ship for pelagic sites.

For processing, each sample was vacuum filtered on to a 47-mm diameter GF/F filter. During filtration, aluminum foil was used to cover the filtration funnel to prevent contamination from airborne microplastic particles. After filtration, filters were dried under vacuum pressure and then stored in 50-mm petri dishes. Following filtration of all three replicates, the filtrate was collected and then re-filtered through a GF/F filter as a control for contamination from the plastic vacuum funnel or potentially airborne microplastics.

Microplastic counting involved visual inspection of the entire GF/F in a similar manner to methods described in Hanvey et al. (2017). Visual enumeration was conducted under a stereo microscope with ~100x magnification, and microplastics were classified into one of three categories: fibers, fragments, or beads. For all categories, plastics were defined as observed

objects with apparent artificial colors, so as to not enumerate plastics potentially contributed from the sampling bottle itself. Fibers were defined as smooth, long plastics with consistent diameters. Fragments were defined as plastics with irregularly sharp or jagged edges. Beads were defined as spherical plastics. Although we did not measure microplastic size, this technique likely allowed us to reliably quantify microplastics as small as ~300 μm (Hanvey et al. 2017). During enumeration, GF/Fs remained covered in the petri dish to minimize potential for contamination from the air. Following enumeration of both experimental and control samples, fibers, fragments, and beads enumerated in the controls were subtracted from the experimental microplastic densities for each plastic type and from each replicate. One location (BK-1) had two control replicates, which were averaged for each plastic type and then subtracted from the experimental samples. Results are reported as the average number of microplastics/L.

Benthic biological samples

At each littoral site, periphyton and macroinvertebrates were collected for relative abundance estimates and food web analysis by wading and snorkeling.

Benthic algal collection

At each littoral site, we haphazardly selected three rocks representative of local substrate. A plastic stencil was used to define a surface area of each rock from which we scraped a standardized 14.5 cm^2 patch of periphyton. Samples were preserved with Lugol's solution and stored in plastic scintillation vials. Additional periphyton was collected in composite from each site for fatty acid and stable isotope analysis.

Periphyton taxonomic identification and enumeration was performed by subsampling 10 µL aliquots from each preserved sample. For all 10 µL aliquots, cells, filaments, and colonies were counted, for the entire subsample, until at least 300 cells were identified for a given sampling replicate. If the first aliquot contained less than 300 cells, we counted additional subsamples until we reached at least 300 cells in total. In instances when 300 cells were counted before finishing a subsample, we still counted the entire aliquot. Taxa were classified into broad categories consistent with Baikal algal taxonomy (Izhboldina 2007), using coarse groupings to capture general patterns in relative algal abundance. As a result, algal groups consisted of diatoms, *Ulothrix*, *Spirogyra*, and the green algal Order Tetrasporales.

Benthic invertebrate collection

At each littoral site, three kick-net samples were collected for assessment of benthic community composition and abundance. Using a D-net, we collected macroinvertebrates by flipping over 1-3 rocks, and then sweeping five times in a left-to-right motion across approximately 1 m. After the series of sweeps, the catch was rinsed into a plastic bucket. For each replicate, bucket contents were concentrated using a 64-µm mesh and placed in glass jars with 40% ethanol (vodka; the only preservative available to us at the time) for preservation and refrigerated at 4°C aboard the research vessel. The 40% ethanol preservative was replaced with ~80% ethanol upon return to the lab within 24 to 48 hours, and samples were stored at ~4°C.

Separate collections were conducted for invertebrate fatty acid and stable isotope analyses. Invertebrates were collected using a D-net in a similar fashion as the community enumeration. Additional invertebrates were also collected by hand. Collected organisms were then live-sorted,

identified to species, and frozen at -20°C at the field station. The samples were later transferred to the lab in the US via a Dewar flask with dry ice.

Invertebrate taxonomic identification and enumeration were performed under a stereo microscope. All invertebrates were identified to species with the exception of juveniles (Takhteev and Didorenko (2015) for amphipods; Sitnikova (2012) for mollusks; Table 2). All samples contained oligochaetes and polychaetes, but due to poor preservation, these taxa were not counted. Six samples of the 42 collected were not well-preserved and were excluded from further analyses, in order to reduce errors in identification. KD-1 and LI-1 were the only sites with 1 sample counted. BK-2 and KD-2 each had two samples counted.

Food web characterization

To characterize littoral food webs, we analyzed carbon and nitrogen stables isotopes as well as fatty acid profiles for periphyton and macroinvertebrates. Prior to isotopic and fatty acid analysis, periphyton and macroinvertebrate samples were lyophilized for ~24 hours, homogenized to powder, and then weighed.

Stable isotope analysis

Measurements of $\delta^{15}N$ and $\delta^{13}C$ were performed on an elemental analyzer-isotope ratio mass spectrometer (EA-IRMS; Finnigan DELTAplus XP, Thermo Scientific) at the Large Lakes Observatory, University of Minnesota Duluth. The EA-IRMS was calibrated against certified reference materials including L-glutamic acid (NIST SRM 8574), low organic soil and sorghum flour (standards B-2153 and B-2159 from Elemental Micro-analysis Ltd., Okehampton, UK) and

372 in-house standards (acetanilide and caffeine). Replicate analyses of external standards showed a
373 mean standard deviation of 0.06 ‰ and 0.09 ‰, for $\delta^{13}C$ and $\delta^{15}N$, respectively.
374
375 *Fatty acid analysis*
376 Following freeze-drying, samples were transferred to 10 mL glass centrifuge vials, and 2 mL of
377 100% chloroform was added to each under nitrogen gas. Samples remained in chloroform
378 overnight at -80°C. Fatty acid extractions generally involved three phases: (1) 100% chloroform
379 extraction, (2) chloroform-methanol extraction, and (3) fatty acid methylation. Fatty acid
380 extraction methods were adapted from Schram et al. (2018).
381
382 After overnight chloroform extraction, samples underwent a chloroform-methanol extraction
383 three times. To each sample, we added 1 mL cooled 100% methanol, 1 mL chloroform:methanol
384 solution (2:1), and 0.8 mL 0.9% NaCl solution. Samples were inverted three times and sonicated
385 on ice for 10 minutes. Next, samples were vortexed for 1 minute, and centrifuged for 5 minutes
386 (3,000 rpm) at 4°C. Using a double pipette technique, the lower organic layer was removed and
387 kept under nitrogen. After the third extraction, samples were evaporated under nitrogen flow, and
388 resuspended in 1.5 mL chloroform and stored at -20°C overnight.
389
390 Once resuspended in chloroform, 1 mL of chloroform extract was transferred to a glass
391 centrifuge tube with a glass syringe as well as an internal standard of 4 µL of 19-carbon fatty
392 acid. Samples were then evaporated under nitrogen, and then 1 mL of toluene and 2 mL of 1%
393 sulfuric acid-methanol was added. The vial was closed under nitrogen gas and then incubated in
394 50°C water bath for 16 hours. After incubation, samples were removed from the bath, allowed to
395 reach room temperature and stored on ice. Next, we performed a potassium carbonate-hexane

extraction twice. To each sample, we added 2 mL of 2% potassium bicarbonate and 5 mL of 100% hexane, inverting the capped vial so as to mix the solution. Samples were centrifuged for 3 minutes (1,500 rpm) at 4°C. The upper hexane layer was then removed and placed in a vial to evaporate under nitrogen flow. Once almost evaporated, 1 mL of 100% hexane was added and stored in a glass amber autosampler vial for GC/MS quantification. GC/MS quantification was performed with a Shimadzu QP2020 GC/MS following Schram et al. (2018).

Statistical analyses

Total phosphorus, nitrate, ammonium, microplastic abundance and density, total PPCP concentration, and $\delta^{15}N$ values in macroinvertebrate tissues were log-transformed and regressed against log-transformed IDW population using a linear model. Analytically, log-transforming made sites comparable, as values spanned three orders of magnitude. Physically, we assumed that sewage indicators were likely subject to exponential processes (e.g., mixing, diffusion), and log-transforming the data should linearize the relationships between predictor and response variables. Residuals were assessed for normality and homogeneity of variance.

To assess if benthic community composition was associated with increasing sewage indicators, periphyton and macroinvertebrate abundance data were each analyzed with a consistent multivariate workflow. First, replicates were averaged, and taxonomic groups representing less than 1% of the inter-site community were removed from analysis, in order to reduce the influence of rare species on results. Second, community compositions for both periphyton and macroinvertebrates were visualized using non-metric multidimensional scaling (NMDS) with a Bray-Curtis similarity metric. Periphyton community compositions were calculated as relative

proportions, whereas invertebrate abundances were grouped at the genus-level and then square-root transformed to minimize influence of more abundant taxa. Visual inspection of the NMDS plot suggested that sites generally tended to separate by increasing PPCP concentrations and IDW population (see Table 2). To test whether sites' benthic communities significantly differed with increasing PPCP concentration and IDW population, we first used k-mediods, also known as Partitioning Around the Mediods (PAM; Kaufman and Rousseeuw 2005), clustering to identify an optimal number of groupings (Figure S1). For this process, we iterated through multiple numbers of clusters (i.e., 1 to 10) and calculated the within-group-sum-of-squares (wss) and average silhouette width. We identified the optimal number of groups when wss decreased most markedly and when silhouette width was greatest (i.e., the elbow method) (Johnson and Wichern 2007). To confirm the optimal number as determined by non-hierarchical PAM clustering, we also used Weighted Pair-Group Centroid Clustering (WPGMC) as a hierarchical approach (Sneath and Sokal 1973), which corrects for clusters that may not be strongly discriminated regardless of how many samples are assigned to a given cluster (Legendre and Legendre 2012). We then performed two permutational multivariate analyses of variance (PERMANOVA; Anderson 2001) with 999 permutations: the first where community compositions were responses to the groups identified through clustering and the second where community compositions were responses to the continuous IDW population. Unlike traditional multivariate analyses of variance (MANOVA), PERMANOVA does not require assumptions of multivariate normality (Anderson 2001). When significant differences were identified, post-hoc SIMPER analysis (Clarke 1993) was performed following the PERMANOVA to identify which taxonomic groups contributed to 85% of the cumulative variance that most influenced site separation.

To assess whether benthic food webs restructured with increasing sewage indicator concentrations, fatty acid data were analyzed in a manner similar to periphyton and macroinvertebrate abundance data. First, species' fatty acid profiles were visualized by performing NMDS with Bray-Curtis similarity for all organisms' relative fatty acid abundance (Figure S2). This technique broadly demonstrated that, as expected, interspecific variation in fatty acid composition was greater than intraspecific variation. The same pattern was observed for all fatty acids quantified as well as solely essential fatty acids (EFAs; Figure S2). Together, these NMDS plots suggested that periphyton fatty acids at sites differentiated based on sewage indicator concentrations, which was likely a reflection of differences in periphyton community composition (Taipale et al. 2013). Among all taxa and sites, 18:3ω3, 18:1ω9, and 20:5ω3 had the highest coefficients of variation, enabling comparisons between sites. These fatty acids tend to be associated with filamentous green algae (i.e., 18:3ω3 and 18:1ω9) and diatoms (i.e., 20:5ω3). To increase the robustness of our analysis, we expanded our approach to include major fatty acids within each taxonomic group, including 18:2ω6 (abundant in green algae); 16:1ω7 and 14:0 (abundant in diatoms); and 16:0 (abundant in both green algae and diatoms) (Taipale et al. 2013). To evaluate how relative fatty acid abundance may relate to sewage pollution, we assessed patterns among these seven fatty acids with both multivariate and univariate approaches. Within a multivariate framework, we created two NMDS plots with Bray-Curtis similarity, one just with primary producer (Figure S5) and the other with macroinvertebrate (Figure S6) fatty acid profiles. Because multivariate patterns suggested fatty acid profiles may relate to sewage pollution, we regressed a filamentous:diatom fatty acid ratio (Equation 2)

$$(2)\ \frac{18{:}3\omega3\% + 18{:}1\omega9\% + 18{:}2\omega6\% + 16{:}0\%}{20{:}5\omega3\% + 16{:}1\omega7\% + 16{:}0\% + 14{:}0\%}$$

against log-transformed PPCP concentrations using a linear model. Additionally, we evaluated how three essential fatty acids (18:3ω3, 18:2ω6, and 20:5ω3), lipids thought to accumulate in biological systems, may differ in abundance across the sewage gradient. Therefore, we similarly regressed the ratio of $\frac{18:3\omega3\% + 18:2\omega6\%}{20:5\omega3\%}$ against log-transformed PPCP concentrations using a linear model.

All analyses were conducted in the R statistical environment (R Core Team 2019), using the tidyverse (Wickham et al. 2019), factoextra (Kassambara and Mundt 2019), cluster (Maechler et al. 2019), pvclust (Suzuki et al. 2019), ggrepel (Slowikowski 2019), viridis (Garnier 2018), fs (Hester and Wickham 2019), spdplyr (Sumner 2019), janitor (Firke 2020), sf (Pebesma 2018), ggpubr (Kassambara 2019), ggtext (Wilke 2020), OpenStreetMap (Fellows and Stotz 2019), cowplot (Wilke 2019), and vegan (Oksanen et al. 2019) packages. All data, including .kml files used to calculate IDW metric, are publicly available from the Environmental Data Initiative repository (Meyer et al. 2020), and all R scripts are available from the GitHub repository of this project's Open Science Framework account (Meyer et al. 2015).

Results

Water samples

Nearshore water nitrate ($R^2 = 0.01$, $p = 0.68$), ammonium ($R^2 = 0.17$, $p = 0.11$), total phosphorus ($R^2 = 0.14$, $p = 0.14$), and chlorophyll a ($R^2 = 0.11$, $p = 0.20$) concentrations were not significantly correlated with IDW population (Figure 3). Total PPCP ($R^2 = 0.26$, $p = 0.04$) concentrations were significantly related with IDW population (Figure 3). In the littoral zone, PPCPs detected included caffeine, 1,7-dimethylxanthine/paraxanthine (main human metabolite

488 of caffeine), cotinine (main human metabolite of nicotine), and acetaminophen/paracetamol
489 (Table 3). Other PPCPs, including carbamazepine, diphenhydramine, thiabendazole,
490 amphetamine, methamphetamine, MDA, MDMA, morphine, phenazone, sulfachloropyridazine,
491 sulfamethazine, sulfadimethoxine, sulfamethazole, trimethoprim, and cimetidine, were not
492 detected.
493
494 Microplastics were detected in samples from both littoral and pelagic sites. Bead microplastics
495 were only detected near Listvyanka. Fibers (mean = 0.85 microplastics/L, std dev = 1.21
496 microplastics/L) and fragments (mean = 0.83 microplastics/L, std dev = 1.35 microplastics/L)
497 were the most abundant types of microplastics across all sites, whereas beads were relatively rare
498 (mean = 0.08 microplastics/L, std dev = 0.31 microplastics/L). Total microplastic densities were
499 not significantly correlated with IDW population ($R^2 = 0.01$, $p = 0.65$; Figure 3), although more
500 types of microplastics were generally observed near areas with higher IDW population values,
501 such as Listvyanka.
502
503 *Benthic biological samples*
504 *Periphyton*
505 Major taxonomic groupings of periphyton consisted of diatoms, *Tetrasporales* spp., *Spirogyra*
506 spp., and *Ulothrix* spp. K-mediods (Figures S1a; S2a) and WPGMC (Figure S3a) cluster
507 analyses of periphyton abundance demonstrated two groupings capture most variance, and visual
508 inspection of relative periphyton community abundance NMDS suggested groupings were
509 related to IDW population values (Figure 4). PERMANOVA results demonstrated that
510 periphyton communities were significantly different based on IDW population groupings ($R^2 =$

511 0.52, p = 0.001) and the continuous IDW population (R^2 = 0.43, p = 0.001). Post-hoc SIMPER
512 results suggested that these differences were primarily associated with sites that had higher
513 *Ulothrix* spp. and *Spirogyra* spp. relative abundance. Additionally, sites with high IDW
514 populations had lower diatom relative abundance in comparison to sites with low and moderate
515 IDW populations.
516
517 *Macroinvertebrates*
518 Taxonomic groupings included five amphipod genera: *Eulimnogammarus*, *Poekilogammarus*,
519 *Cryptoropus*, *Brandtia and Pallasea*; six mollusk families: Planorbidae, Valvatidae, Baicaliidae,
520 Benedictidae, Acroloxidae, Maackia; flatworms; caddisflies; and leeches (summarized in Table
521 S1). K-mediod cluster analysis of macroinvertebrate community composition suggested 2 or 3
522 major groupings would capture most variance (Figure S1b; S2b), whereas WPGMC analyses
523 suggested 2 groupings would enable all sites except for one to be assigned a cluster (S3b).
524 Because both forms of hierarchical and non-hierarchical clustering suggested two groupings as
525 optimal, we proceeded using two groupings. Visual inspection of NMDS suggested clusters were
526 related to IDW population (Figure 5). PERMANOVA results supported the hypothesis that
527 macroinvertebrate communities significantly differed both among our IDW population groupings
528 (R^2 = 0.19, p = 0.02) and along our continuous gradient of increasing IDW population (R^2 =
529 0.19, p = 0.02). Post-hoc SIMPER analyses suggested that *Poekilogammarus*,
530 *Eulimnogammarus*, Valvatidae, Caddisflies, *Brandtia*, Baicaliidae, Planorbidae, *Cryptoropus*,
531 and flatworms contributed the greatest differences between high and moderate/low IDW
532 population groupings (see Table 2).
533

Food web characterization: stable isotopes and fatty acids

Among periphyton and amphipod samples, $\delta^{13}C$ values ranged from -19.5 to -9.5 ‰ (Figure 6). Among periphyton samples, $\delta^{15}N$ values ranged from 0.77 to 3.76 ‰, whereas amphipod $\delta^{15}N$ values ranged from 6.42 to 7.92 ‰.

For grazers, $\delta^{15}N$ significantly increased with IDW population ($p = 0.01$; Figure 3, Figure 6). Periphyton $\delta^{15}N$ signatures did not significantly increase with IDW population ($p = 0.27$). In contrast, $\delta^{13}C$ concentrations were not related with IDW population for either periphyton or macroinvertebrates.

With respect to fatty acids, macroinvertebrates tended to be characterized by mono-unsaturated fatty acids (MUFAs) and long-chain (i.e. ≥ 20-Carbons) polyunsaturated fatty acids (LCPUFAs), whereas periphyton tended to be characterized by short-chain (i.e., 16- and 18-Carbons) polyunsaturated fatty acids (SCPUFAs) (Table 3). When comparing proportions within taxa across the sewage gradient, periphyton SCPUFA proportion tended to increase (Figure S4) and periphyton SAFA proportions generally decreased. In contrast, benthic macroinvertebrate fatty acid class proportions tended to remain consistent across the entire gradient (Figure S4).

For both periphyton and grazers, our analyses focused mainly on the fatty acids consistently associated with filamentous green algae (i.e., 18:3ω3, 18:1ω9, 18:2ω6, and 16:0) as well as diatoms (i.e., 20:5ω3, 16:1ω7, 14:0, and 16:0). For periphyton, the ratio of green filamentous:diatom-associated fatty acids significantly increased with an increasing PPCP concentration ($R^2 = 0.62$; $p = 0.04$, Figure 7; S5) but not with an increasing IDW population ($p =$

557 0.08). Amphipod fatty acid ratios were not significantly related with either increasing IDW
558 population or increasing PPCP concentrations (Figure 7; S6). When focusing solely on the
559 essential fatty acids 18:3ω3, 18:2ω6, and 20:5ω3, the same pattern was observed in both
560 periphyton ($R^2 = 0.73$; $p = 0.02$) and amphipods (Figure 7).
561
562 **Discussion**
563 Our combined results corroborate previous findings (e.g., Timoshkin et al., 2016; 2018) that
564 sewage pollution is entering Lake Baikal's nearshore area and likely is responsible for changes in
565 nearshore benthic communities. Unlike previous studies, we were able to incorporate highly
566 specific indicators of sewage pollution and food web structure to offer direct, quantitative
567 relationships between human development and ecological responses.
568
569 *Relating human settlements to sewage indicator concentrations*
570 In agreement with our expectations, some sewage pollution indicators in the nearshore of Lake
571 Baikal were associated with size of and distance from human settlements. Total PPCP,
572 macroinvertebrate $\delta^{15}N$, and, to some degree, total phosphorus concentrations increased with
573 IDW population. These sewage gradients created by highly localized settlements are noteworthy
574 considering that Baikal's shoreline, including our study area, is largely free of lakeside
575 development (Moore et al. 2009). Furthermore, the use of sewage-associated indicators, such as
576 PPCPs and $\delta^{15}N$, proved necessary for defining sewage gradients. The use of nutrients as
577 indicators alone would not reveal sewage pollution gradients, since nutrients were not strongly
578 correlated with IDW population and could come from diverse sources. For example, melting
579 permafrost in Lake Baikal's watershed (Anisimov and Reneva 2006) and the Selenga River basin

(Tornqvist et al. 2014) as well as climate-driven changes in mixing processes (Swann et al. 2020) have the potential to contribute substantial nutrient loadings to the nearshore. While nutrients also could be contributed by agriculture (Powers et al. 2016), atmospheric deposition (Galloway et al. 2004; Monteith et al. 2007; Stoddard et al. 2016), and changing terrestrial plant communities (Moran et al. 2012), these are not currently known to be major sources of elevated nutrients in the Baikal watershed, relative to sewage (Timoshkin et al., 2016, Timoshkin et al., 2018) and permafrost melt (Anisimov & Reneva, 2006).

This is the first known study to detect PPCPs in Lake Baikal, a voluminous lake in a largely unpopulated watershed. We detected PPCPs nearshore but not at our three offshore sites, suggesting that sewage inputs in Baikal become diluted as pollutants move out of the nearshore area. More generally, these results are important for lake monitoring, as PPCPs are robust indicators of sewage pollution. Beyond Lake Baikal, these data are important for understanding PPCPs' prevalence in lakes, as lakes have remained less represented in the PPCP literature in comparison to lotic and subsurface systems (Meyer et al. 2019). This literature imbalance creates opportunities to assess how PPCPs, and sewage pollution more broadly, may lead to differing ecological responses in lotic and lentic systems. As lakes tend to have longer hydraulic residence times relative to rivers and streams, pollutants may be more prone to accumulate (Yang et al. 2018; Meyer et al. 2019). In the case of our data, comparing contemporaneous littoral and pelagic PPCP concentrations revealed littoral-pelagic sewage gradients, as PPCPs were degraded, metabolized or accumulated by biota, preserved within sediments, or diluted to undetectable concentrations. In the context of the entire lake, analyses of sediments have shown how PPCPs can remain within lake systems for decades, thereby enabling researchers to

603 reconstruct histories of wastewater pollution in a system (Czekalski et al. 2015; Yang et al.
604 2018).
605
606 Investigating PPCP concentrations across limnic environments could also establish how
607 ecological communities respond differently not only to sewage but also to the PPCPs themselves.
608 While we focus on PPCPs as indicators of sewage, previous studies have shown that PPCPs,
609 even at concentrations we observed in Lake Baikal, can elicit biological responses from
610 physiological (e.g., del Rey et al. 2011; Feijão et al. 2020) and behavioral (e.g., Brodin et al.
611 2013; Dzieweczynski et al. 2016) levels to food webs (e.g., Lagesson et al. 2016; Richmond et
612 al. 2018) and ecosystems (e.g., Rosi-Marshall et al. 2013; Richmond et al. 2019; Robson et al.
613 2020). Although our study was not designed to evaluate the ecotoxicological effects of PPCPs
614 themselves, future studies could potentially address effects of PPCPs on nearshore Baikal biota
615 by using *in situ* sewage gradients as a guide.
616
617 In contrast to PPCP concentrations and $\delta^{15}N$ values, microplastics were not associated with IDW
618 population and may be poor proxies for sewage pollution in Lake Baikal. Additionally,
619 microplastics may originate from non-sewage sources, such as agriculture (Steinmetz et al. 2016)
620 and fish nets (Eerkes-Medrano et al. 2015). Because of their long degradation time (Brandon et
621 al. 2016), microplastics can indicate accumulated pollution, which likely enables wider
622 distribution from nearshore inputs to the offshore (Fischer et al. 2016; Hendrickson et al. 2018).
623 Unlike microplastic concentrations identified in Lake Hovsgol (Free et al. 2014), Lake Superior
624 (Hendrickson et al. 2018), or Lake Erie (Eriksen et al. 2013), microplastic concentrations in
625 Baikal, as quantified by our methods, may be poor proxies for capturing pollution from

626 seasonally varying human populations. It is worth noting that since the time of our field
627 sampling, evidence has accumulated that our methods likely dramatically underestimated
628 microplastic abundance (Wang and Wang 2018; Brandon et al. 2020), and there is potential for
629 the microplastics themselves to cause deleterious ecological responses. While we focus here on
630 microplastics as an indicator of sewage pollution, microplastics are increasingly shown to disrupt
631 food web dynamics by altering grazing patterns (Green 2016) and providing carbon substrate for
632 microbial growth (Romera-Castillo et al. 2018). Recent investigations of microplastics in Lake
633 Baikal near Bolshie Koty (BK) used analogous methods and measured similarly low
634 concentrations (Karnaukhov et al. 2020). When considering Lake Baikal's large volume,
635 Karnaukov et al. (2020) noted that the number of plastic pieces may well exceed those observed
636 in other lakes, such as Lake Hovsgol. Together these growing uncertainties suggest that
637 microplastic pollution in Baikal and elsewhere deserves increased attention.
638
639 *Relating sewage indicators with benthic algal communities*
640 Congruent with our hypotheses, increasing sewage indicators tended to be associated with higher
641 relative abundance of filamentous taxa in periphyton. Previous studies investigating Baikal's
642 periphyton composition noted that areas adjacent to human development often had increased
643 abundance of filamentous algae such as *Ulothrix* and *Spirogyra* (Timoshkin et al. 2016, 2018).
644 Lake Baikal's southwestern shore historically experiences short *Ulothrix* blooms in late August
645 (Kozhov 1963), potentially confounding sewage signals with an annually occurring
646 phenomenon. Our data are consistent with the results of Timoshkin et al. (2016) and show that
647 relative abundance of filamentous algae is greatest near areas of higher lakeside development.
648

While community composition shifted with increasing sewage indicator concentrations, periphyton $\delta^{15}N$ values did not differ along our transect. Previous studies in marine (Gartner et al. 2002; Savage and Elmgren 2004; Risk et al. 2009) and freshwater (Wayland and Hobson 2001; Camilleri and Ozersky 2019) systems have highlighted how sewage-associated $\delta^{15}N$ can increase in algal samples and even throughout the food web. Like PPCPs in our study, $\delta^{15}N$ values are often most enriched near the source of sewage pollution and can decrease over several kilometers (Savage and Elmgren 2004), with concentrations varying based on species-specific uptake rates and advective, dispersive, and diffusive transport (Gartner et al. 2002). While previous studies using $\delta^{15}N$ signatures in macroalgae and vascular macrophytes have successfully tracked sewage gradients (Cole et al. 2004), periphyton $\delta^{15}N$ as a sewage indicator potentially can be confounded by terrestrial $\delta^{15}N$ contributions such as through agricultural runoff (Chang et al. 2012). In our study, periphyton $\delta^{15}N$ signatures may be explained by periphyton's typically high cell turnover rates (e.g., days; Swamikannu and Hoagland 1989) dampening isotopic patterns, $\delta^{15}N$-accumulating algal taxa being grazed more readily by macroinvertebrates (Rosenberger et al. 2008), or co-limitation dynamics between ammonium and nitrate (York et al. 2007; Piñón-Gimate et al. 2009).

Fatty acid analyses suggested that changes in periphyton community composition altered the nutritional quality of periphyton across the pollution gradient. Periphyton fatty acid profiles from sites with higher sewage pollution had higher levels of 18:3ω3, 18:1ω9, 18:2ω6, and 16:0 relative to 20:5ω3, 16:1ω7, 16:0, and 14:0 fatty acids. This pattern likely reflects the higher abundance of green algae relative to diatoms (Iverson et al. 2004; Osipova et al. 2009; Taipale et al. 2013; Galloway and Winder 2015; Shishlyannikov et al. 2018), which we observed from our

672 periphyton community composition analysis (Figure 3). Together, our periphyton composition
673 and fatty acid results suggest that Baikal's nearshore periphyton communities near human
674 lakeside developments are more dominated by filamentous green algae, and therefore, have
675 lower nutritional content.
676
677 Among the array of fatty acids synthesized in algal communities, essential fatty acids (EFAs) are
678 most likely to be taxonomically associated with, and influenced by, changing community
679 composition. EFAs are a subgroup of polyunsaturated fatty acids (PUFAs) that are prone to
680 accumulating in organisms (see Kelly & Scheibling, 2012). Among the eight common EFAs
681 (Taipale et al. 2013), 18:3ω3, 18:2ω6, and 20:5ω3 had the highest coefficients of variation
682 between sites. Because these three EFAs demonstrated the greatest variation between sites, our
683 analyses focused on how their relative abundances related to PPCP concentrations and IDW
684 populations. The fatty acids 18:3ω3 and 18:2ω6 have been previously associated with
685 filamentous algae, such as Baikalian *Ulothrix* (Osipova et al. 2009), whereas 20:5ω3 have
686 previously been associated with Baikalian diatoms (Shishlyannikov et al. 2018). Comparing the
687 ratio of filamentous green algae to diatoms could therefore function as proxy for each algal
688 taxon's relative abundance and potentially offer insights into feeding patterns for the grazers.
689
690 *Relating sewage indicators with macroinvertebrate feeding guilds*
691 In assessing benthic consumer communities' responses to changing periphyton, our data suggest
692 macroinvertebrate guilds reshape with increasing sewage pollution. Our results support the
693 general conclusion of Timoshkin et al. (2016) that Baikalian mollusk abundance tends to
694 decrease with increasing sewage pollution. Decreased mollusk abundance may have several

causes, including low tolerance for increased concentrations of PPCPs or other components of sewage (e.g., Hollingsworth et al. 2002, Timoshkin et al. 2016), inability to consume filamentous algae (Mazzella and Russo 1989), or filamentous algae not offering the proper nutrition (Lowe and Hunter 1988). In contrast to mollusks, amphipods were generally prevalent at all littoral sites, regardless of sewage indicator concentrations. *Brandtia* spp. was the only amphipod genus less abundant with sewage indicator signals. This genus tends to be associated with endemic sponges (Taakhteev & Didorenko, 2015), which may also be decreasing in abundance near areas of lakeside development (Timoshkin et al., 2016). *Eulimnogammarus* spp., one of the most speciose Baikal genera (Takhteev and Didorenko 2015), was prevalent at all sites, and $\delta^{15}N$ values in its tissue increased slightly but significantly with increasing IDW population. Unlike periphyton, amphipods' increasing $\delta^{15}N$ values may relate to amphipods having longer cellular turnover rates (e.g., weeks; McIntyre and Flecker 2006) relative to periphyton. Consequently, amphipods' enhanced $\delta^{15}N$ values suggest that sewage-derived nutrients are being incorporated into the food web. While we did not test amphipod tissues for other sewage indicators such as PPCPs and microplastics, the potential for PPCPs to bioaccumulate and biomagnify in food webs has been recently demonstrated, with ecological ramifications remaining uncertain (Lagesson et al., 2016; Richmond et al., 2018). These combined results suggest that mollusk abundance and amphipod $\delta^{15}N$ values may be longer-term indicators of sewage pollution in Baikal.

In contrast to variation in $\delta^{15}N$ values, amphipod fatty acid profiles did not differ markedly between sites (Figure 7). Amphipods from all collected sites expressed consistent 20:5ω3 signatures relative to 18:3ω3 and 18:2ω6. Consumers usually accumulate fatty acids from their food source. Yoshii's (1999) study as well as our own stable isotope data suggest that Baikal's

718 benthic, littoral amphipods are likely a combination of grazers and omnivores. Because fatty acid
719 profiles in amphipods largely reflected fatty acid signatures in periphyton, our data suggest that
720 amphipods likely continue grazing on periphyton, despite the food resource changing in
721 community composition and nutritional content. As a consequence, amphipods may be
722 compensating for the shifting nutritional quality of periphyton through at least two potential
723 mechanisms. First, amphipods may selectively consume diatoms as opposed to filamentous
724 algae, meaning diatom relative abundance could decrease both from increased grazing and lesser
725 efficiency at taking up nutrients relative to filamentous taxa. Second, amphipods themselves
726 (e.g., Desvilettes et al. 1997; Castell et al. 2004) or heterotrophic symbionts (Klein Breteler et al.
727 1999; Veloza et al. 2006; Hiltunen et al. 2017) may upgrade fatty acids by investing energy to
728 convert C18 fatty acids to C20 fatty acids. Regardless of the exact mechanism, our data suggest
729 that food web interactions would change with increasing sewage pollution and may imply a net
730 energetic cost through amphipods' differential grazing patterns.
731
732 *Conclusions*
733 Over the past decade, Lake Baikal has shown signs of nearshore eutrophication, despite the
734 pelagic zone remaining ultra-oligotrophic. While Baikal receives nutrients from multiple sources,
735 sewage-specific indicators used in this study implicate wastewater pollution as one of the
736 sources. Our results corroborate work by Timoshkin et al. (2016, 2018), demonstrating how
737 patchy hot spots of lakeside development at Baikal can create gradients in sewage concentrations
738 and ecological responses. Unlike previous studies, our approach pairs community abundance
739 data (i.e., periphyton and macroinvertebrate counts) and nuanced dietary tracers (i.e., fatty acids)
740 to assess benthic community and food web consequences of sewage pollution. While sewage

741 pollution may lead to changing resources for macroinvertebrate grazers, Baikal's amphipods
742 appear to be compensating either (1) by selectively grazing on diatoms or (2) by consuming less
743 desirable food and upgrading fatty acids. In both cases, our results suggest shifting community
744 interactions and may imply a net energetic cost for amphipods, as they expend energy either by
745 foraging selectively for diatoms or by catabolizing certain essential fatty acids.
746
747 *Future trajectories: a call for increased nearshore monitoring*
748 Our results underscore the importance of nearshore monitoring in detecting sewage pollution in
749 large lakes. Lake Baikal is considered ultra-oligotrophic based on pelagic sampling (Yoshida et
750 al. 2003; O'Donnell et al. 2017), but nearshore hot spots of eutrophication are developing
751 throughout the lake (Timoshkin et al. 2016, 2018). While pelagic samples are representative of
752 the lake's overall status, nearshore sampling aids managers in identifying pollution loading
753 before the entire system is affected (Jacoby et al. 1991; Lambert et al. 2008; Hampton et al.
754 2011). Beyond Baikal, several large, deep, oligotrophic lakes have likewise experienced
755 localized sewage pollution with nearshore biological responses, despite pelagic measurements
756 suggesting oligotrophic status (e.g., Jacoby et al. 1991, Rosenberger et al. 2008; Hampton et al.,
757 2011). Once eutrophication of the open water has occurred, mitigation can involve complex
758 socio-economic factors (Carpenter et al. 1999), require system-specific information (Jeppesen et
759 al. 2005), and necessitate long-term strategies (Tong et al. 2020). Because nutrients may enter
760 systems from numerous sources, incorporating sewage specific indicators, such as PPCPs, may
761 be necessary. PPCP sampling has the potential to not only identify sewage-associated nutrient
762 pollution but also assess heterogeneities in sewage loading along a shoreline. When PPCP data
763 are paired with co-located benthic community composition and food web data, managers can

764 take system-specific actions to mitigate ecological consequences before sewage concentrations
765 are detected throughout the lake. Across larger spatial and temporal scales, these paired PPCP-
766 biological samples have potential to offer a synoptic view of the impacts of sewage pollution,
767 enabling regional and local monitoring to coordinate mitigation strategies
768

Works Cited

Anderson, M. J. 2001. A new method for non-parametric multivariate analysis of variance. Austral Ecology **26**: 32–46. doi:10.1111/j.1442-9993.2001.01070.pp.x

Andersson, E., and A.-K. Brunberg. 2006. Inorganic nutrient acquisition in a shallow clearwater lake – dominance of benthic microbiota. Aquatic Sciences **68**: 172–180. doi:10.1007/s00027-006-0805-x

Anisimov, O., and S. Reneva. 2006. Permafrost and Changing Climate: The Russian Perspective. Ambio **35**: 169–175.

Barnes, D. K. A., F. Galgani, R. C. Thompson, and M. Barlaz. 2009. Accumulation and fragmentation of plastic debris in global environments. Philos Trans R Soc Lond B Biol Sci **364**: 1985–1998. doi:10.1098/rstb.2008.0205

Bendz, D., N. A. Paxéus, T. R. Ginn, and F. J. Loge. 2005. Occurrence and fate of pharmaceutically active compounds in the environment, a case study: Höje River in Sweden. Journal of Hazardous Materials **122**: 195–204. doi:10.1016/j.jhazmat.2005.03.012

Brandon, J. A., A. Freibott, and L. M. Sala. 2020. Patterns of suspended and salp-ingested microplastic debris in the North Pacific investigated with epifluorescence microscopy. Limnology and Oceanography Letters **5**: 46–53. doi:10.1002/lol2.10127

Brandon, J., M. Goldstein, and M. D. Ohman. 2016. Long-term aging and degradation of microplastic particles: Comparing in situ oceanic and experimental weathering patterns. Marine Pollution Bulletin **110**: 299–308. doi:10.1016/j.marpolbul.2016.06.048

Brodin, T., J. Fick, M. Jonsson, and J. Klaminder. 2013. Dilute Concentrations of a Psychiatric Drug Alter Behavior of Fish from Natural Populations. Science **339**: 814–815. doi:10.1126/science.1226850

Camilleri, A. C., and T. Ozersky. 2019. Large variation in periphyton δ13C and δ15N values in the upper Great Lakes: Correlates and implications. Journal of Great Lakes Research **45**: 986–990. doi:10.1016/j.jglr.2019.06.003

Carpenter, S. R., D. Ludwig, and W. A. Brock. 1999. Management of Eutrophication for Lakes Subject to Potentially Irreversible Change. Ecological Applications **9**: 751–771. doi:10.2307/2641327

Castell, J. D., E. J. Kennedy, S. M. C. Robinson, G. J. Parsons, T. J. Blair, and E. Gonzalez-Duran. 2004. Effect of dietary lipids on fatty acid composition and metabolism in juvenile green sea urchins (Strongylocentrotus droebachiensis). Aquaculture **242**: 417–435. doi:10.1016/j.aquaculture.2003.11.003

Chang, H.-Y., S.-H. Wu, K.-T. Shao, and others. 2012. Longitudinal variation in food sources and their use by aquatic fauna along a subtropical river in Taiwan. Freshwater Biology **57**: 1839–1853. doi:10.1111/j.1365-2427.2012.02843.x

Clarke, K. R. 1993. Non-parametric multivariate analyses of changes in community structure. Australian Journal of Ecology **18**: 117–143. doi:https://doi.org/10.1111/j.1442-9993.1993.tb00438.x

Cole, M. L., I. Valiela, K. D. Kroeger, and others. 2004. Assessment of a delta15N isotopic method to indicate anthropogenic eutrophication in aquatic ecosystems. J. Environ. Qual. **33**: 124–132. doi:10.2134/jeq2004.1240

Costanzo, S. D., M. J. O'Donohue, W. C. Dennison, N. R. Loneragan, and M. Thomas. 2001. A New Approach for Detecting and Mapping Sewage Impacts. Marine Pollution Bulletin **42**: 149–156. doi:10.1016/S0025-326X(00)00125-9

Craine, J. M., A. J. Elmore, L. Wang, and others. 2018. Isotopic evidence for oligotrophication of terrestrial ecosystems. Nature Ecology & Evolution **2**: 1735–1744. doi:10.1038/s41559-018-0694-0

Czekalski, N., R. Sigdel, J. Birtel, B. Matthews, and H. Bürgmann. 2015. Does human activity impact the natural antibiotic resistance background? Abundance of antibiotic resistance genes in 21 Swiss lakes. Environment International **81**: 45–55. doi:10.1016/j.envint.2015.04.005

D'Alessio, M., S. Onanong, D. D. Snow, and C. Ray. 2018. Occurrence and removal of pharmaceutical compounds and steroids at four wastewater treatment plants in Hawai'i and their environmental fate. Science of The Total Environment **631–632**: 1360–1370. doi:10.1016/j.scitotenv.2018.03.100

Dalsgaard, J., M. St. John, G. Kattner, D. Müller-Navarra, and W. Hagen. 2003. Fatty acid trophic markers in the pelagic marine environment, p. 225–340. *In* Advances in Marine Biology. Elsevier.

Desvilettes, Ch., G. Bourdier, and J. Ch. Breton. 1997. On the occurrence of a possible bioconversion of linolenic acid into docosahexaenoic acid by the copepod *Eucyclops serrulatus* fed on microalgae. J Plankton Res **19**: 273–278. doi:10.1093/plankt/19.2.273

Dzieweczynski, T. L., B. A. Campbell, and J. L. Kane. 2016. Dose-dependent fluoxetine effects on boldness in male Siamese fighting fish. Journal of Experimental Biology **219**: 797–804. doi:10.1242/jeb.132761

Eerkes-Medrano, D., R. C. Thompson, and D. C. Aldridge. 2015. Microplastics in freshwater systems: A review of the emerging threats, identification of knowledge gaps and prioritisation of research needs. Water Research **75**: 63–82. doi:10.1016/j.watres.2015.02.012

Eriksen, M., S. Mason, S. Wilson, C. Box, A. Zellers, W. Edwards, H. Farley, and S. Amato. 2013. Microplastic pollution in the surface waters of the Laurentian Great Lakes. Marine Pollution Bulletin **77**: 177–182. doi:10.1016/j.marpolbul.2013.10.007

Feijão, E., R. Cruz de Carvalho, I. A. Duarte, and others. 2020. Fluoxetine Arrests Growth of the Model Diatom Phaeodactylum tricornutum by Increasing Oxidative Stress and Altering Energetic and Lipid Metabolism. Front Microbiol **11**. doi:10.3389/fmicb.2020.01803

Fellows, I., and using the Jm. library by J. P. Stotz. 2019. OpenStreetMap: Access to Open Street Map Raster Images,.

Firke, S. 2020. janitor: Simple Tools for Examining and Cleaning Dirty Data,.

844 Fischer, E. K., L. Paglialonga, E. Czech, and M. Tamminga. 2016. Microplastic pollution in lakes and
845 lake shoreline sediments – A case study on Lake Bolsena and Lake Chiusi (central Italy).
846 Environmental Pollution **213**: 648–657. doi:10.1016/j.envpol.2016.03.012
847 Focazio, M. J., D. W. Kolpin, K. K. Barnes, E. T. Furlong, M. T. Meyer, S. D. Zaugg, L. B. Barber, and
848 M. E. Thurman. 2008. A national reconnaissance for pharmaceuticals and other organic
849 wastewater contaminants in the United States - II) Untreated drinking water sources. SCIENCE
850 OF THE TOTAL ENVIRONMENT **402**: 201–216. doi:10.1016/j.scitotenv.2008.02.021
851 Free, C. M., O. P. Jensen, S. A. Mason, M. Eriksen, N. J. Williamson, and B. Boldgiv. 2014. High-levels
852 of microplastic pollution in a large, remote, mountain lake. Marine Pollution Bulletin **85**: 156–
853 163. doi:10.1016/j.marpolbul.2014.06.001
854 Galloway, A. W. E., and M. Winder. 2015. Partitioning the Relative Importance of Phylogeny and
855 Environmental Conditions on Phytoplankton Fatty Acids. PLOS ONE **10**: e0130053.
856 doi:10.1371/journal.pone.0130053
857 Galloway, J. N., F. J. Dentener, D. G. Capone, and others. 2004. Nitrogen Cycles: Past, Present, and
858 Future. Biogeochemistry **70**: 153–226. doi:10.1007/s10533-004-0370-0
859 Garnier, S. 2018. viridis: Default Color Maps from “matplotlib,.”
860 Gartner, A., P. Lavery, and A. J. Smit. 2002. Use of delta N-15 signatures of different functional forms of
861 macroalgae and filter-feeders to reveal temporal and spatial patterns in sewage dispersal. Mar.
862 Ecol.-Prog. Ser. **235**: 63–73. doi:10.3354/meps235063
863 Green, D. S. 2016. Effects of microplastics on European flat oysters, Ostrea edulis and their associated
864 benthic communities. Environmental Pollution **216**: 95–103. doi:10.1016/j.envpol.2016.05.043
865 Guzzo, M. M., G. D. Haffner, S. Sorge, S. A. Rush, and A. T. Fisk. 2011. Spatial and temporal
866 variabilities of δ13C and δ15N within lower trophic levels of a large lake: implications for
867 estimating trophic relationships of consumers. Hydrobiologia **675**: 41–53. doi:10.1007/s10750-
868 011-0794-1

Hadwen, W. L., and S. E. Bunn. 2005. Food web responses to low-level nutrient and^ 1^ 5N-tracer additions in the littoral zone of an oligotrophic dune lake. Limnology and Oceanography **50**: 1096.

Hampton, S. E., S. C. Fradkin, P. R. Leavitt, and E. E. Rosenberger. 2011. Disproportionate importance of nearshore habitat for the food web of a deep oligotrophic lake. Marine and Freshwater Research **62**: 350. doi:10.1071/MF10229

Hampton, S. E., S. McGowan, T. Ozersky, and others. 2018. Recent ecological change in ancient lakes. Limnology and Oceanography **63**: 2277–2304. doi:10.1002/lno.10938

Hanvey, J. S., P. J. Lewis, J. L. Lavers, N. D. Crosbie, K. Pozo, and B. O. Clarke. 2017. A review of analytical techniques for quantifying microplastics in sediments. Anal. Methods **9**: 1369–1383. doi:10.1039/C6AY02707E

Hendrickson, E., E. C. Minor, and K. Schreiner. 2018. Microplastic Abundance and Composition in Western Lake Superior As Determined via Microscopy, Pyr-GC/MS, and FTIR. Environ. Sci. Technol. **52**: 1787–1796. doi:10.1021/acs.est.7b05829

Hester, J., and H. Wickham. 2019. fs: Cross-Platform File System Operations Based on “libuv,.”

Hiltunen, M., M. Honkanen, S. Taipale, U. Strandberg, and P. Kankaala. 2017. Trophic upgrading via the microbial food web may link terrestrial dissolved organic matter to Daphnia. J Plankton Res **39**: 861–869. doi:10.1093/plankt/fbx050

Hollingsworth, R. G., J. W. Armstrong, and E. Campbell. 2002. Caffeine as a repellent for slugs and snails. Nature **417**: 915–916. doi:10.1038/417915a

Interfax-Tourism. 2018. Байкал с января по август 2018 года посетили 1,2 миллиона туристов (1.2 million tourists vistied Baikal from January through August 2018). Interfax-Tourism, October 25

Iverson, S. J., C. Field, W. D. Bowen, and W. Blanchard. 2004. Quantitative Fatty Acid Signature Analysis: A New Method of Estimating Predator Diets. Ecological Monographs **74**: 211–235. doi:10.1890/02-4105

Izhboldina, L. A. 2007. Guide and Key to Benthic and Periphyton Algae of Lake Baikal (meio- and macrophytes) with Brief Notes on Their Ecology, Nauka-Centre.

Jacoby, J. M., D. D. Bouchard, and C. R. Patmont. 1991. Response of Periphyton to Nutrient Enrichment in Lake Chelan, WA. Lake and Reservoir Management **7**: 33–43. doi:10.1080/07438149109354252

Jeppesen, E., M. Søndergaard, J. P. Jensen, and others. 2005. Lake responses to reduced nutrient loading – an analysis of contemporary long-term data from 35 case studies. Freshwater Biology **50**: 1747–1771. doi:10.1111/j.1365-2427.2005.01415.x

Johnson, R. A., and D. V. Wichern. 2007. Applied Multivariate Statistical Analysis, 6th ed. Prentice Hall.

Karnaukhov, D., S. Biritskaya, E. Dolinskaya, M. Teplykh, N. Silenko, Y. Ermolaeva, and E. Silow. 2020. POLLUTION BY MACRO- AND MICROPLASTIC OF LARGE LACUSTRINE ECOSYSTEMS IN EASTERN ASIA. Pollution Research **2**: 353–355.

Karnjanapiboonwong, A., A. N. Morse, J. D. Maul, and T. A. Anderson. 2010. Sorption of estrogens, triclosan, and caffeine in a sandy loam and a silt loam soil. Journal of Soils and Sediments **10**: 1300–1307. doi:10.1007/s11368-010-0223-5

Kassambara, A. 2019. ggpubr: “ggplot2” Based Publication Ready Plots,.

Kassambara, A., and F. Mundt. 2019. factoextra: Extract and Visualize the Results of Multivariate Data Analyses,.

Kaufman, L., and P. J. Rousseeuw. 2005. Finding Groups in Data: An Introduction to Cluster Analysis, 1st Edition. Wiley-Interscience.

Kelly, J. R., and R. E. Scheibling. 2012. Fatty acids as dietary tracers in benthic food webs. Marine Ecology Progress Series **446**: 1–22. doi:10.3354/meps09559

Klein Breteler, W. C. M., N. Schogt, M. Baas, S. Schouten, and G. W. Kraay. 1999. Trophic upgrading of food quality by protozoans enhancing copepod growth: role of essential lipids. Marine Biology **135**: 191–198. doi:10.1007/s002270050616

Klein, S., E. Worch, and T. P. Knepper. 2015. Occurrence and Spatial Distribution of Microplastics in River Shore Sediments of the Rhine-Main Area in Germany. Environ. Sci. Technol. **49**: 6070–6076. doi:10.1021/acs.est.5b00492

Kolpin, D. W., E. T. Furlong, M. T. Meyer, E. M. Thurman, S. D. Zaugg, L. B. Barber, and H. T. Buxton. 2002. Pharmaceuticals, Hormones, and Other Organic Wastewater Contaminants in U.S. Streams, 1999−2000: A National Reconnaissance. Environmental Science & Technology **36**: 1202–1211. doi:10.1021/es011055j

Kozhov, M. M. 1963. Lake Baikal and its Life, Springer Science & Business Media.

Kozhova, O. M., and L. R. Izmest'eva. 1998. Lake Baikal: Evolution and Biodiversity, Backhuys Publishers.

Kravtsova, L. S., L. A. Izhboldina, I. V. Khanaev, and others. 2014. Nearshore benthic blooms of filamentous green algae in Lake Baikal. Journal of Great Lakes Research **40**: 441–448. doi:10.1016/j.jglr.2014.02.019

Lagesson, A., J. Fahlman, T. Brodin, J. Fick, M. Jonsson, P. Byström, and J. Klaminder. 2016. Bioaccumulation of five pharmaceuticals at multiple trophic levels in an aquatic food web - Insights from a field experiment. Science of The Total Environment **568**: 208–215. doi:10.1016/j.scitotenv.2016.05.206

Lambert, D., A. Cattaneo, and R. Carignan. 2008. Periphyton as an early indicator of perturbation in recreational lakes. Can. J. Fish. Aquat. Sci. **65**: 258–265. doi:10.1139/f07-168

Legendre, P., and L. Legendre. 2012. Numerical Ecology, 3rd ed. Elsevier.

Li, J., C. Green, A. Reynolds, H. Shi, and J. M. Rotchell. 2018. Microplastics in mussels sampled from coastal waters and supermarkets in the United Kingdom. Environmental Pollution **241**: 35–44. doi:10.1016/j.envpol.2018.05.038

Lorenzen, C. J. 1967. Determination of Chlorophyll and Pheo-Pigments: Spectrophotometric Equations1. Limnology and Oceanography **12**: 343–346. doi:https://doi.org/10.4319/lo.1967.12.2.0343

944 Lowe, R. L., and R. D. Hunter. 1988. Effect of Grazing by Physa integra on Periphyton Community
945 Structure. Journal of the North American Benthological Society **7**: 29–36. doi:10.2307/1467828
946 Maechler, M., P. Rousseeuw, A. Struyf, M. Hubert, and K. Hornik. 2019. cluster: Cluster Analysis Basics
947 and Extensions,.
948 Mazzella, L., and G. F. Russo. 1989. Grazing effect of two Gibbula species (Mollusca,
949 Archaeogastropoda) on the epiphytic community of Posidonia oceanica leaves.
950 McIntyre, P. B., and A. S. Flecker. 2006. Rapid turnover of tissue nitrogen of primary consumers in
951 tropical freshwaters. Oecologia **148**: 12–21. doi:10.1007/s00442-005-0354-3
952 Meyer, M. F., T. Ozersky, K. H. Woo, and others. 2020. A unified dataset of co-located sewage pollution,
953 periphyton, and benthic macroinvertebrate community and food web structure from Lake Baikal
954 (Siberia).doi:10.6073/PASTA/76F43144015EC795679BAC508EFA044B
955 Meyer, M. F., S. M. Powers, and S. E. Hampton. 2019. An Evidence Synthesis of Pharmaceuticals and
956 Personal Care Products (PPCPs) in the Environment: Imbalances among Compounds, Sewage
957 Treatment Techniques, and Ecosystem Types. Environ. Sci. Technol. **53**: 12961–12973.
958 doi:10.1021/acs.est.9b02966
959 Meyer, M., T. Ozersky, K. Woo, A. W. E. Galloway, M. R. Brousil, and S. Hampton. 2015. Baikal Food
960 Webs.doi:10.17605/OSF.IO/9TA8Z
961 Monteith, D. T., J. L. Stoddard, C. D. Evans, and others. 2007. Dissolved organic carbon trends resulting
962 from changes in atmospheric deposition chemistry. Nature **450**: 537–540.
963 doi:10.1038/nature06316
964 Moore, J. W., D. E. Schindler, M. D. Scheuerell, D. Smith, and J. Frodge. 2003. Lake eutrophication at
965 the urban fringe, Seattle region, USA. AMBIO: A Journal of the Human Environment **32**: 13–18.
966 Moore, M. V., S. E. Hampton, L. R. Izmest'eva, E. A. Silow, E. V. Peshkova, and B. K. Pavlov. 2009.
967 Climate Change and the World's "Sacred Sea"-Lake Baikal, Siberia. Bioscience **59**: 405–417.
968 doi:10.1525/bio.2009.59.5.8

969 Moran, P. W., S. E. Cox, S. S. Embrey, R. L. Huffman, T. D. Olsen, and S. C. Fradkin. 2012. Sources and
970 Sinks of Nitrogen and Phosphorus in a Deep, Oligotrophic Lake, Lake Crescent, Olympic
971 National Park, Washington. US Geological Survey.
972 O'Donnell, D. R., P. Wilburn, E. A. Silow, L. Y. Yampolsky, and E. Litchman. 2017. Nitrogen and
973 phosphorus colimitation of phytoplankton in Lake Baikal: Insights from a spatial survey and
974 nutrient enrichment experiments. Limnology and Oceanography **62**: 1383–1392.
975 doi:10.1002/lno.10505
976 Oksanen, J., F. G. Blanchet, M. Friendly, and others. 2019. vegan: Community Ecology Package,.
977 Osipova, S., L. Dudareva, N. Bondarenko, A. Nasarova, N. Sokolova, L. Obolkina, O. Glyzina, and O.
978 Timoshkin. 2009. Temporal variation in fatty acid composition of Ulothrix zonata (Chlorophyta)
979 from ice and benthic communities of Lake Baikal. Phycologia **48**: 130–135.
980 Ozersky, T., E. A. Volkova, N. A. Bondarenko, O. A. Timoshkin, V. V. Malnik, V. M. Domysheva, and
981 S. E. Hampton. 2018. Nutrient limitation of benthic algae in Lake Baikal, Russia. Freshwater
982 Science **37**: 472–482. doi:10.1086/699408
983 Parsons, T. R., and J. D. H. Strickland. 1963. Discussion of spectrophotometric determination of marine-
984 plant pigments, with revised equations for ascertaining chlorophylls and carotenoids. Journal of
985 Marine Research.
986 Pebesma, E. 2018. Simple Features for R: Standardized Support for Spatial Vector Data. The R Journal
987 **10**: 439–446. doi:10.32614/RJ-2018-009
988 Piñón-Gimate, A., M. F. Soto-Jiménez, M. J. Ochoa-Izaguirre, E. García-Pagés, and F. Páez-Osuna. 2009.
989 Macroalgae blooms and δ15N in subtropical coastal lagoons from the Southeastern Gulf of
990 California: Discrimination among agricultural, shrimp farm and sewage effluents. Marine
991 Pollution Bulletin **58**: 1144–1151. doi:10.1016/j.marpolbul.2009.04.004
992 Powers, S. M., T. W. Bruulsema, T. P. Burt, and others. 2016. Long-term accumulation and transport of
993 anthropogenic phosphorus in three river basins. Nature Geoscience **9**: 353–356.
994 doi:10.1038/ngeo2693

R Core Team. 2019. R: A Language and Environment for Statistical Computing,.

del Rey, Z. R., E. F. Granek, and B. A. Buckley. 2011. Expression of HSP70 in Mytilus californianus following exposure to caffeine. Ecotoxicology **20**: 855–861. doi:10.1007/s10646-011-0649-6

Richmond, E. K., E. J. Rosi, A. J. Reisinger, B. R. Hanrahan, R. M. Thompson, and M. R. Grace. 2019. Influences of the antidepressant fluoxetine on stream ecosystem function and aquatic insect emergence at environmentally realistic concentrations. Journal of Freshwater Ecology **34**: 513–531. doi:10.1080/02705060.2019.1629546

Richmond, E. K., E. J. Rosi, D. M. Walters, J. Fick, S. K. Hamilton, T. Brodin, A. Sundelin, and M. R. Grace. 2018. A diverse suite of pharmaceuticals contaminates stream and riparian food webs. Nature Communications **9**: 4491. doi:10.1038/s41467-018-06822-w

Risk, M. J., B. E. Lapointe, O. A. Sherwood, and B. J. Bedford. 2009. The use of δ15N in assessing sewage stress on coral reefs. Marine Pollution Bulletin **58**: 793–802. doi:10.1016/j.marpolbul.2009.02.008

Robson, S. V., E. J. Rosi, E. K. Richmond, and M. R. Grace. 2020. Environmental concentrations of pharmaceuticals alter metabolism, denitrification, and diatom assemblages in artificial streams. Freshwater Science **39**: 256–267. doi:10.1086/708893

Romera-Castillo, C., M. Pinto, T. M. Langer, X. A. Álvarez-Salgado, and G. J. Herndl. 2018. Dissolved organic carbon leaching from plastics stimulates microbial activity in the ocean. Nat Commun **9**: 1–7. doi:10.1038/s41467-018-03798-5

Rosenberger, E. E., S. E. Hampton, S. C. Fradkin, and B. P. Kennedy. 2008. Effects of shoreline development on the nearshore environment in large deep oligotrophic lakes. Freshwater Biology **53**: 1673–1691. doi:10.1111/j.1365-2427.2008.01990.x

Rosi-Marshall, E. J., D. W. Kincaid, H. A. Bechtold, T. V. Royer, M. Rojas, and J. J. Kelly. 2013. Pharmaceuticals suppress algal growth and microbial respiration and alter bacterial communities in stream biofilms. Ecological Applications **23**: 583–593. doi:10.1890/12-0491.1

1020 Rosi-Marshall, E. J., and T. V. Royer. 2012. Pharmaceutical Compounds and Ecosystem Function: An
1021 Emerging Research Challenge for Aquatic Ecologists. Ecosystems **15**: 867–880.
1022 doi:10.1007/s10021-012-9553-z
1023 Sargent, J. R., and S. Falk-Petersen. 1988. The lipid biochemistry of calanoid copepods. Hydrobiologia
1024 **167–168**: 101–114. doi:10.1007/BF00026297
1025 Savage, C., and R. Elmgren. 2004. MACROALGAL (FUCUS VESICULOSUS) δ15N VALUES TRACE
1026 DECREASE IN SEWAGE INFLUENCE. Ecological Applications **14**: 517–526. doi:10.1890/02-
1027 5396
1028 Schram, J. B., J. N. Kobelt, M. N. Dethier, and A. W. E. Galloway. 2018. Trophic Transfer of Macroalgal
1029 Fatty Acids in Two Urchin Species: Digestion, Egestion, and Tissue Building. Front. Ecol. Evol.
1030 **6**. doi:10.3389/fevo.2018.00083
1031 Shishlyannikov, S. M., A. A. Nikonova, Y. S. Bukin, and A. G. Gorshkov. 2018. Fatty acid trophic
1032 markers in Lake Baikal phytoplankton: A comparison of endemic and cosmopolitan diatom-
1033 dominated phytoplankton assemblages. Ecological Indicators **85**: 878–886.
1034 doi:10.1016/j.ecolind.2017.11.052
1035 Sitnikova, T. Ya. 2012. Определитель брюхоногих моллюсков бухты Большие Коты (юго-западное
1036 побережье озера Байкал) [Key of the Gastropod Molluscs in the Bay of Bolshie Koty (South-
1037 West shoreline of Lake Baikal)], Irkutsk State University.
1038 Slowikowski, K. 2019. ggrepel: Automatically Position Non-Overlapping Text Labels with "ggplot2,."
1039 Smith, V. H., G. D. Tilman, and J. C. Nekola. 1999. Eutrophication: impacts of excess nutrient inputs on
1040 freshwater, marine, and terrestrial ecosystems. Environmental Pollution **100**: 179–196.
1041 doi:10.1016/S0269-7491(99)00091-3
1042 Sneath, P. H. A., and R. R. Sokal. 1973. Numerical Taxonomy: The Principles and Practice of Numerical
1043 Classification, W. H. Freeman.

1044 Steinmetz, Z., C. Wollmann, M. Schaefer, and others. 2016. Plastic mulching in agriculture. Trading
1045 short-term agronomic benefits for long-term soil degradation? Science of The Total Environment
1046 **550**: 690–705. doi:10.1016/j.scitotenv.2016.01.153
1047 Stoddard, J. L., J. Van Sickle, A. T. Herlihy, J. Brahney, S. Paulsen, D. V. Peck, R. Mitchell, and A. I.
1048 Pollard. 2016. Continental-Scale Increase in Lake and Stream Phosphorus: Are Oligotrophic
1049 Systems Disappearing in the United States? Environ. Sci. Technol. **50**: 3409–3415.
1050 doi:10.1021/acs.est.5b05950
1051 Sumner, M. D. 2019. spdplyr: Data Manipulation Verbs for the Spatial Classes,.
1052 Suzuki, R., Y. Terada, and H. Shimodaira. 2019. pvclust: Hierarchical Clustering with P-Values via
1053 Multiscale Bootstrap Resampling,.
1054 Swamikannu, X., and K. D. Hoagland. 1989. Effects of Snail Grazing on the Diversity and Structure of a
1055 Periphyton Community in a Eutrophic Pond. Can. J. Fish. Aquat. Sci. **46**: 1698–1704.
1056 doi:10.1139/f89-215
1057 Swann, G. E. A., V. N. Panizzo, S. Piccolroaz, and others. 2020. Changing nutrient cycling in Lake
1058 Baikal, the world's oldest lake. PNAS **117**: 27211–27217. doi:10.1073/pnas.2013181117
1059 Taipale, S., U. Strandberg, E. Peltomaa, A. W. E. Galloway, A. Ojala, and M. T. Brett. 2013. Fatty acid
1060 composition as biomarkers of freshwater microalgae: analysis of 37 strains of microalgae in 22
1061 genera and in seven classes. Aquatic Microbial Ecology **71**: 165–178. doi:10.3354/ame01671
1062 Takhteev, V. V., and D. I. Didorenko. 2015. Fauna and ecology of amphipods of Lake Baikal: A Training
1063 manual, V.B. Sochava Institute of Geography SB RAS.
1064 Timoshkin, O. A., M. V. Moore, N. N. Kulikova, and others. 2018. Groundwater contamination by
1065 sewage causes benthic algal outbreaks in the littoral zone of Lake Baikal (East Siberia). Journal
1066 of Great Lakes Research. doi:10.1016/j.jglr.2018.01.008
1067 Timoshkin, O. A., D. P. Samsonov, M. Yamamuro, and others. 2016. Rapid ecological change in the
1068 coastal zone of Lake Baikal (East Siberia): Is the site of the world's greatest freshwater

biodiversity in danger? Journal of Great Lakes Research **42**: 487–497. doi:10.1016/j.jglr.2016.02.011

Tong, Y., M. Wang, J. Peñuelas, and others. 2020. Improvement in municipal wastewater treatment alters lake nitrogen to phosphorus ratios in populated regions. Proc Natl Acad Sci USA **117**: 11566–11572. doi:10.1073/pnas.1920759117

Tornqvist, R., J. Jarsjo, J. Pietron, A. Bring, P. Rogberg, S. M. Asokan, and G. Destouni. 2014. Evolution of the hydro-climate system in the Lake Baikal basin. Journal of Hydrology **519**: 1953–1962. doi:10.1016/j.jhydrol.2014.09.074

Turetsky, M. R., R. K. Wieder, C. J. Williams, and D. H. Vitt. 2000. Organic matter accumulation, peat chemistry, and permafrost melting in peatlands of boreal Alberta. Écoscience **7**: 115–122. doi:10.1080/11956860.2000.11682608

Veloza, A. J., F.-L. E. Chu, and K. W. Tang. 2006. Trophic modification of essential fatty acids by heterotrophic protists and its effects on the fatty acid composition of the copepod Acartia tonsa. Marine Biology **148**: 779–788. doi:10.1007/s00227-005-0123-1

Volkova, E. A., N. A. Bondarenko, and O. A. Timoshkin. 2018. Morphotaxonomy, distribution and abundance of *Spirogyra* (Zygnematophyceae, Charophyta) in Lake Baikal, East Siberia. Phycologia **57**: 298–308. doi:10.2216/17-69.1

de Vries, J. 1972. Soil Filtration of Wastewater Effluent and the Mechanism of Pore Clogging. Journal (Water Pollution Control Federation) **44**: 565–573.

Wang, W., and J. Wang. 2018. Investigation of microplastics in aquatic environments: An overview of the methods used, from field sampling to laboratory analysis. TrAC Trends in Analytical Chemistry **108**: 195–202. doi:10.1016/j.trac.2018.08.026

Wayland, M., and K. A. Hobson. 2001. Stable carbon, nitrogen, and sulfur isotope ratios in riparian food webs on rivers receiving sewage and pulp-mill effluents. Can. J. Zool. **79**: 5–15. doi:10.1139/z00-169

Wickham, H., M. Averick, J. Bryan, and others. 2019. Welcome to the tidyverse. Journal of Open Source Software **4**: 1686. doi:10.21105/joss.01686

Wilke, C. O. 2019. cowplot: Streamlined Plot Theme and Plot Annotations for "ggplot2,."

Wilke, C. O. 2020. ggtext: Improved Text Rendering Support for "ggplot2,."

Yang, Y., W. Song, H. Lin, W. Wang, L. Du, and W. Xing. 2018. Antibiotics and antibiotic resistance genes in global lakes: A review and meta-analysis. Environment International **116**: 60–73. doi:10.1016/j.envint.2018.04.011

Yang, Y.-Y., G. S. Toor, P. C. Wilson, and C. F. Williams. 2016. Septic systems as hot-spots of pollutants in the environment: Fate and mass balance of micropollutants in septic drainfields. Science of The Total Environment **566–567**: 1535–1544. doi:10.1016/j.scitotenv.2016.06.043

York, J. K., G. Tomasky, I. Valiela, and D. J. Repeta. 2007. Stable isotopic detection of ammonium and nitrate assimilation by phytoplankton in the Waquoit Bay estuarine system. Limnology and Oceanography **52**: 144–155. doi:10.4319/lo.2007.52.1.0144

Yoshida, T., T. Sekino, M. Genkai-Kato, and others. 2003. Seasonal dynamics of primary production in the pelagic zone of southern Lake Baikal. Limnology **4**: 53–62. doi:10.1007/s10201-002-0089-3

Yoshii, K. 1999. Stable isotope analyses of benthic organisms in Lake Baikal. Hydrobiologia **411**: 145–159.

2016a. Methods for determination of nitrogen-containing matters (with corrections) (Методы определения азотсодержащих веществ (с Поправками)).

2016b. Methods for determination of phosphorus-containing matters (with corrections) (Методы определения фосфорсодержащих веществ).

2017. Nitrate concentration in waters: Photometric methods with Giress reagent following stabilization in a cadmium reducer (Массовая концентрация нитратного азота в водах: Методика измерений фотометрическим методом с реактивом Грисса после восстановления в камиевом редукторе).

Acknowledgments

We would like to thank the faculty, students, staff, and mariners of the Irkutsk State University's Biological Research Institute Biostation for their expert field, taxonomic, and laboratory support; Marianne Moore and Bart De Stasio for helpful advice; the researchers and students of the Siberian Branch of the Russian Academy of Sciences Limnological Institute for expert taxonomic and logistical assistance; Oleg A. Timoshkin, Tatiana Ya. Sitnikova, Irina V. Mekhanikova, Nina A. Bonderenko, Ekaterina Volkova, Yulia Zvereva, Vadim V. Takhteev, Stephanie G. Labou, Stephen L. Katz, Brian P. Lanouette, John R. Loffredo, Alli N. Cramer, Alexander K. Fremier, Erica J. Crespi, Stephen M. Powers, Daniel L. Preston, Gavin L. Simpson, and James J. Elser for offering insights throughout the development of this project. Funding was provided by the National Science Foundation (NSF-DEB-1136637) to S.E.H., a Fulbright Fellowship to M.F.M., a NSF Graduate Research Fellowship to M.F.M. (NSF-DGE-1347973), and the Russian Ministry of Science and Education (N FZZE-2020-0026; FZZE-2020-0023). This work serves as one chapter of M.F.M.'s doctoral dissertation in Environmental and Natural Resource Sciences at Washington State University.

1136

Table 1: Location, depth, temperature and population information for each of the 17 sampling stations. “OS” refers to pelagic locations (i.e., “Offshore”), whereas other site abbreviations refer to littoral sampling locations.

Site	Latitude	Longitude	Depth (m)	Distance to shore (m)	Air Temperature (°C)	Surface Temperature (°C)	Adjacent Population
BK-1	51.90316	105.07404	0.7	10	18	14	80
BK-2	51.90365	105.069	0.9	17.5	19	13	80
BK-3	51.90536	105.0957	0.8	10	18	14	80
BGO-1	52.02693	105.40102	0.9	18	20	13	0
BGO-2	52.0197	105.37707	1.1	14	19	14	600
BGO-3	52.02649	105.43577	0.7	21	18	16	600
OS-1	51.98559	105.47237	900	NA	15	NA	NA
KD-1	51.92646	105.24504	0.8	20.75	23	NA	0
KD-2	51.91807	105.21456	0.9	14.5	23	16	0
MS-1	51.89863	105.15017	0.6	10.5	21	17	0
SM-1	51.87152	104.98006	0.9	11.5	21	15	0
LI-1	51.86825	104.83042	0.6	8.9	19	14	2000

LI-2	51.84626	104.87356	0.8	9.4	21	15	2000
LI-3	51.85407	104.86216	0.7	9.25	19.5	15	2000
EM-1	51.86005	104.93999	0.7	15.5	24.5	14	0
OS-2	51.8553	104.8148	1300	NA	21	NA	NA
OS-3	51.859108	105.0769	1400	5000	NA	14.5	NA

1137

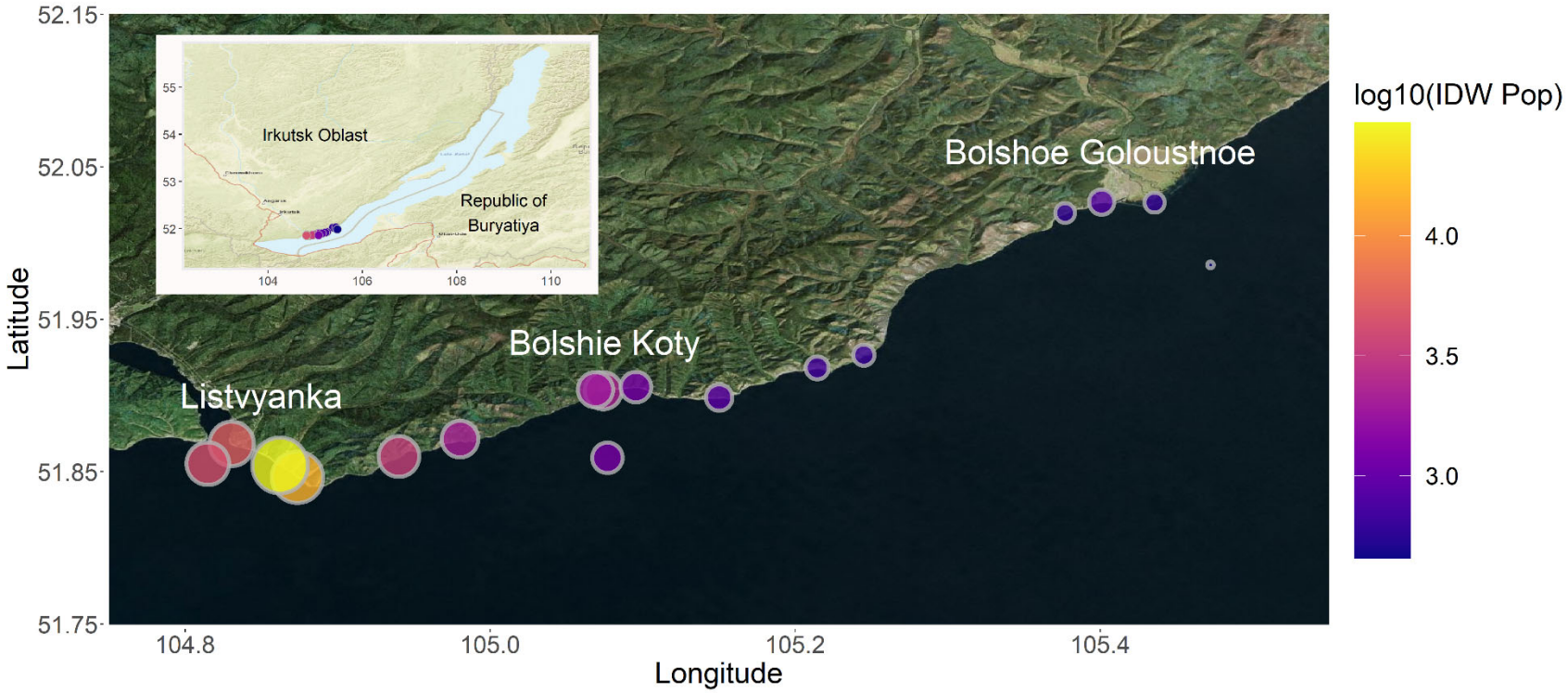

Figure 1: Map of all sampling locations with sites sized and colored by log-transformed IDW population. IDW population was log-transformed so as to make IDW populations across three orders of magnitude more comparable. The entire transect included three developed sites (i.e., Listvyanka, Bolshie Koty, Bolshoe Goloustnoe). Three offshore samples were also collected to compare pelagic sewage signals to those in the littoral. Sampling locations west of Listvyanka are located farther from Listvyanka's centroid, and therefore have lower IDW population values than sites located closer to the centroid. This map was created using the R statistical

1144 environment (R Core Team 2019) and the tidyverse (Wickham et al. 2019), OpenStreeetMap (Fellows and Stotz 2019), ggpubr
1145 (Kassambara 2019), cowplot (Wilke 2019), and ggrepel (Slowikowski 2019) packages.
1146

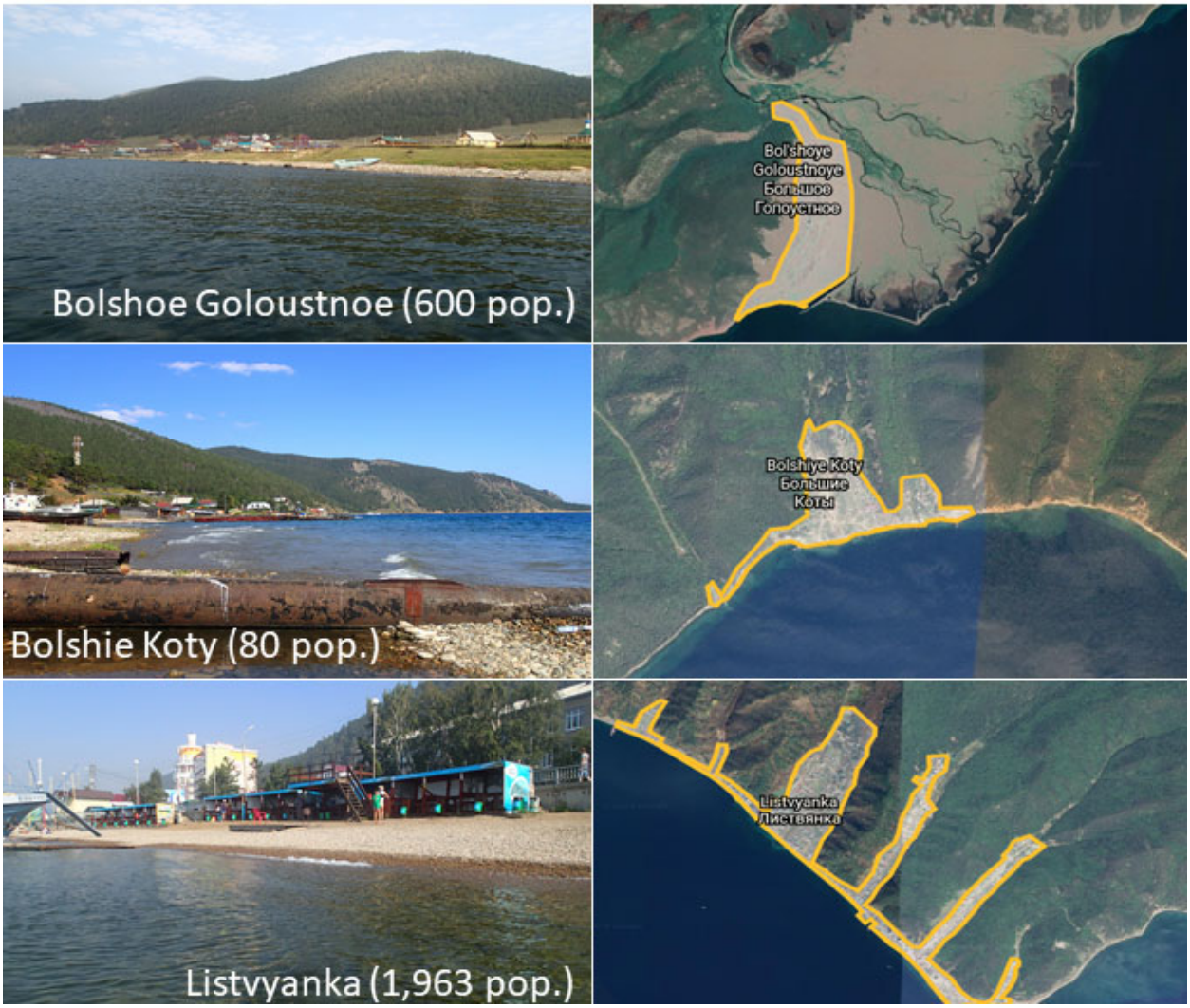

Figure 2: Photographs and Google Earth imagery of each developed area. Photographs were taken by Kara H. Woo and Michael F. Meyer.

Table 2: Average sewage indicator concentrations and densities per sampling location. Caffeine, acetaminophen/paracetamol, paraxanthine, and cotinine detection limits are estimated to be 0.001 µg/L based on a 500 mL sample volume.

Site	NH_4^+ (mg/L)	NO_3^- (mg/L)	Total Phosphorus (mg/L)	Caffeine (µg/L)	Acetaminophen (µg/L)	Paraxanthine (µg/L)	Cotinine (µg/L)	Fragment density (MPs/L)	Fiber density (MPs/L)	Bead density (MPs/L)	IDW population	Categorical IDW population
BK-1	0.003	0.085	0.054	0.011	0.001	0.002	0	0	0.000833	0	2304.039	High
BK-2	0.003	0.085	0.052	0.007	0.001	0	0	0.000952	0.000476	0	1891.558	Mod/Low
BK-3	0.068	0.09	0.045	0.003	0.001	0	0	0.003095	0.00119	0	1231.234	Mod/Low
BGO-1	0.0145	0.085	0.044	0	0.002	0	0	0.00119	0	0	838.5385	Mod/Low
BGO-2	0.001	0.08	0.0385	0	0.001	0	0	0.000238	0.001905	0	611.91	Mod/Low
BGO-3	0.001	0.09	0.044	0.005	0.003	0	0	0	0	0	624.455	Mod/Low
OS-1	0.001	0.085	0.061	0	0.001	0	0.001	0.002381	0	0	455.7733	Mod/Low
KD-1	0.0035	0.065	0.0375	0.003	0.001	0	0	0	0.000476	0	662.4151	Mod/Low
KD-2	0.001	0.1	0.0445	0.001	0.001	0	0	0.000714	0.001905	0	720.5484	Mod/Low
MS-1	0.001	0.09	0.061	0.064	0.035	0.015	0	0	0.000238	0	903.6733	Mod/Low
SM-1	0.001	0.085	0.1475	0.042	0.012	0.005	0	0	0.001667	0	2146.218	Mod/Low
LI-1	0.004	0.08	0.0385	0.05	0.04	0.006	0.002	0.00381	0.000238	0.000714	5403.209	High
LI-2	0.091	0.095	0.0775	0.001	0.007	0	0	0.001429	0.00119	0	14792.51	High
LI-3	0.0035	0.08	0.077	0.027	0.002	0.002	0.003	0.000476	0	0.000714	29511.73	High
EM-1	0.1125	0.185	0.092	0.029	0.014	0.002	0	0	0.000238	0	3389.949	High
OS-2	0.001	0.08	0.078	0.033	0.001	0.004	0.003	0.000238	0.001905	0	4340	High
OS-3	0.001	0.08	0.0795	0.001	0.001	0	0	0	0.002143	0	1221.424	Mod/Low

1151

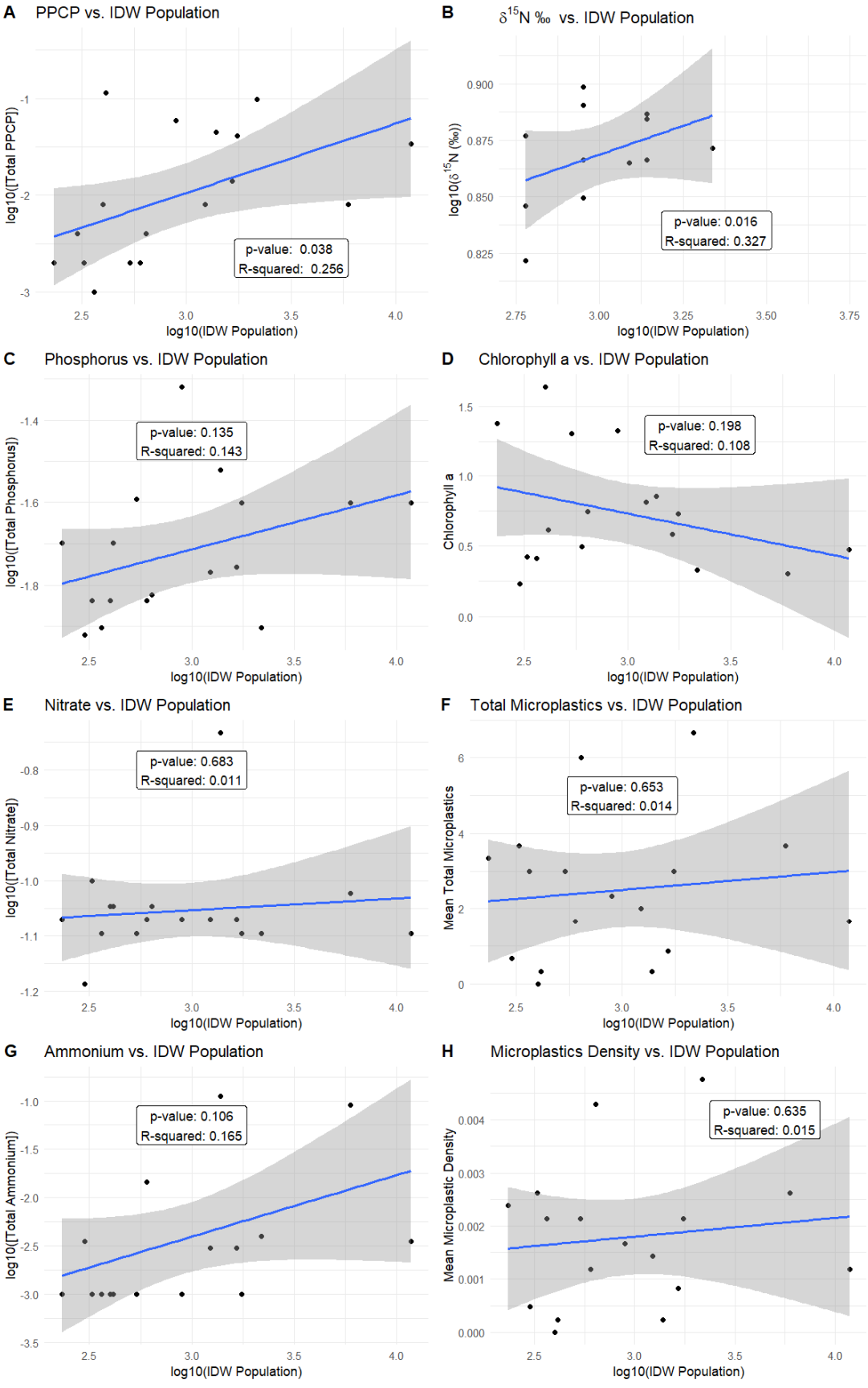
A PPCP vs. IDW Population
log10([Total PPCP])
log10(IDW Population)
p-value: 0.038
R-squared: 0.256
B δ15N ‰ vs. IDW Population
log10(δ15N (‰))
log10(IDW Population)
p-value: 0.016
R-squared: 0.327
C Phosphorus vs. IDW Population
log10([Total Phosphorus])
log10(IDW Population)
p-value: 0.135
R-squared: 0.143
D Chlorophyll a vs. IDW Population
Chlorophyll a
log10(IDW Population)
p-value: 0.198
R-squared: 0.108
E Nitrate vs. IDW Population
log10([Total Nitrate])
log10(IDW Population)
p-value: 0.683
R-squared: 0.011
F Total Microplastics vs. IDW Population
Mean Total Microplastics
log10(IDW Population)
p-value: 0.653
R-squared: 0.014
G Ammonium vs. IDW Population
log10([Total Ammonium])
log10(IDW Population)
p-value: 0.106
R-squared: 0.165
H Microplastics Density vs. IDW Population
Mean Microplastic Density
log10(IDW Population)
p-value: 0.635
R-squared: 0.015

1152

Figure 3: Linear models of total PPCP concentrations (A), macroinvertebrate $\delta^{15}N$ (B), total phosphorus (C), chlorophyll a (D), nitrate (E), total microplastics (F), ammonium (G), and microplastic density (H) regressed against log-transformed inverse distance weighted (IDW) population. Total PPCP concentrations (A) and macroinvertebrate $\delta^{15}N$ (B) produced significant models. Total phosphorus (C), chlorophyll a (D), nitrate (E), total microplastics (F), ammonium (G), and microplastic density (H) did not produce significant models.

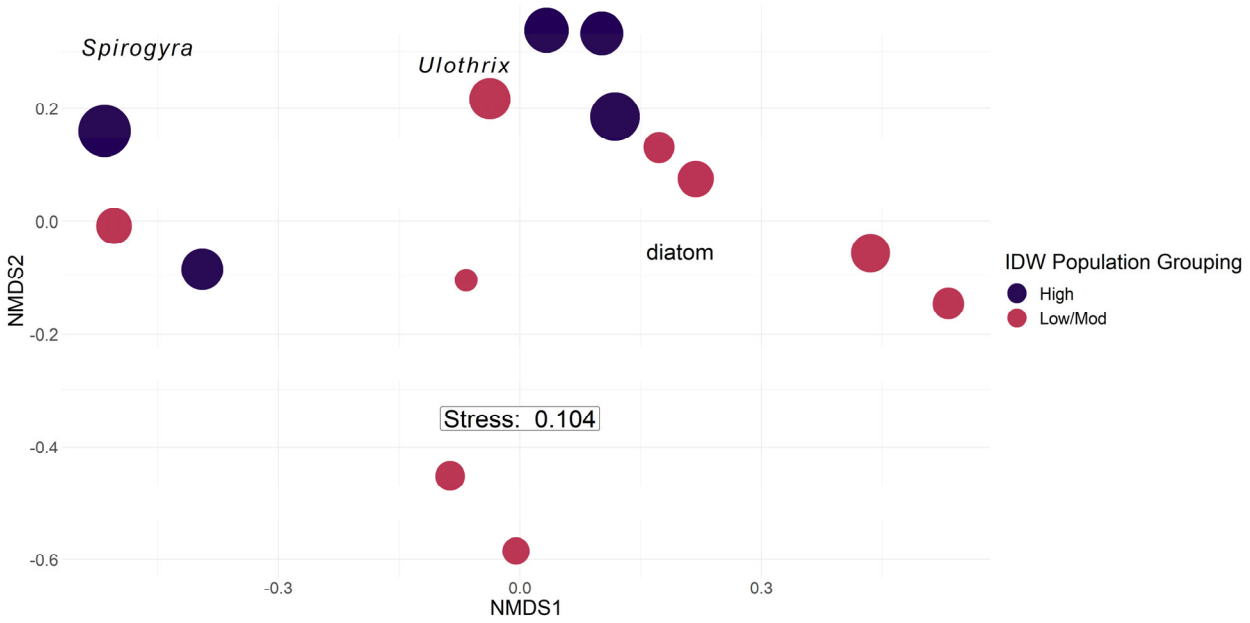

Figure 4: Periphyton abundance NMDS with Bray-Curtis dissimilarity. Points are sized by log10 IDW population and colored by grouped IDW population values. Taxonomic labels represent species scores, which are weighted averages of species contributions from site scores. For periphyton, PERMANOVA ($p = 0.001$) and post-hoc SIMPER results suggested sites with a higher IDW population value tended to be more associated with filamentous algal groupings and separate from sites with moderate and low IDW population values, which were more associated with diatom abundance.

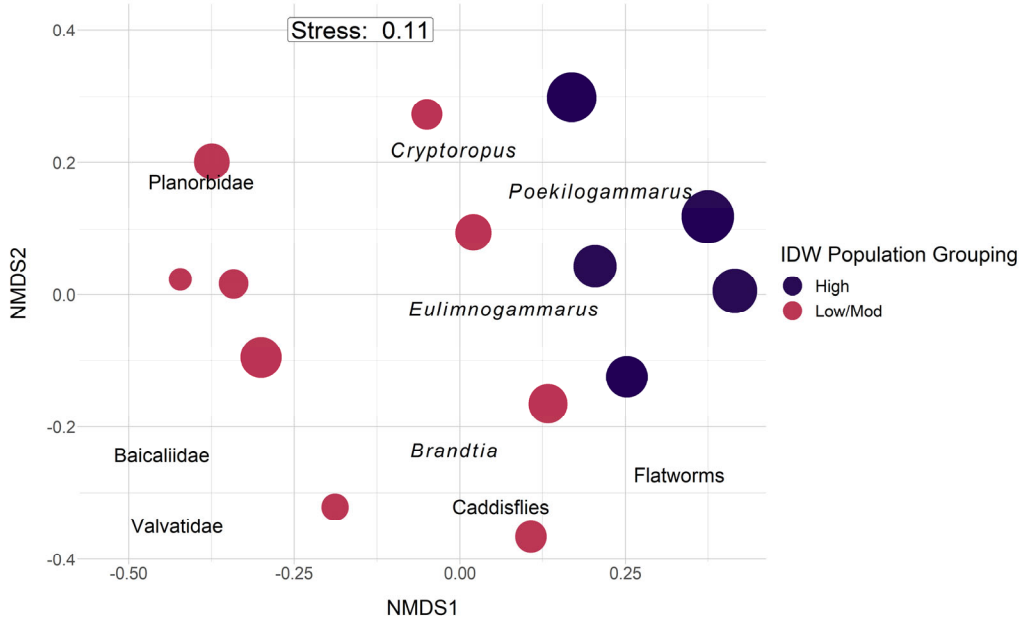

Figure 5: Macroinvertebrate abundance NMDS with Bray-Curtis dissimilarity. Points are sized by log10 IDW population and colored by grouped IDW population values. Taxonomic labels represent species scores, which are weighted averages of species contributions from site scores. For macroinvertebrates, PERMANOVA ($p = 0.02$) and post-hoc SIMPER results suggested sites with a higher IDW population values tended to be associated with amphipod taxa (see Table S1), whereas sites with lower and moderate IDW population values were more associated with increased mollusk abundance (see Table S1).

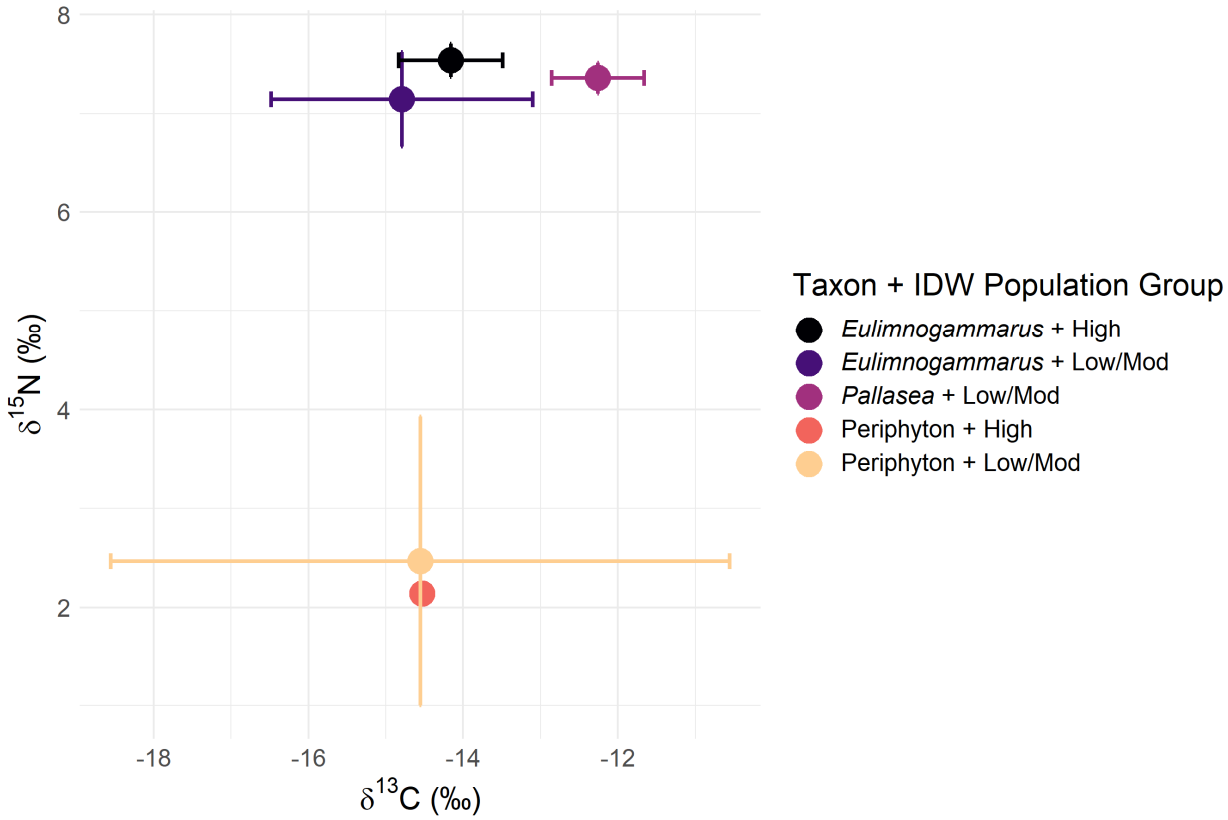

1177

1178

1179 Figure 6: Biplot of mean and standard deviation $\delta^{13}C$ and $\delta^{15}N$ stable isotope values for littoral

1180 amphipods and periphyton, grouped by categorical IDW population (Table 3). In general,

1181 periphyton did not differ in $\delta^{13}C$ or $\delta^{15}N$ signatures with increasing IDW population, whereas

1182 *Eulimnogammarus* amphipods increased in $\delta^{15}N$ signatures with increasing IDW population.

1183 *Pallasea* signatures differed from *Eulimnogammarus* most likely because *Pallasea* tends to

1184 remain in the nearshore area, whereas *Eulimnogammarus* will regularly migrate to deeper zones

1185 (Takhteev & Didorenko, 2015).

1186

Table 3: Mean inter-site fatty acid proportion of each taxon and fatty acid grouping (as defined in table S2).

Taxon	Number of sites	Branched	LCPUFA	MUFA	SAFA	SCPUFA
Draparnaldia spp.	4	0.000	0.012	0.088	0.189	0.710
Eulimnogammarus cyaneus	2	0.002	0.259	0.309	0.248	0.182
Eulimnogammarus verrucosus	6	0.000	0.188	0.385	0.240	0.187
Eulimnogammarus vittatus	6	0.001	0.171	0.371	0.241	0.216
Pallasea cancellus	3	0.001	0.282	0.359	0.187	0.171
Periphyton	7	0.000	0.073	0.092	0.284	0.550
Snail	3	0.002	0.470	0.123	0.194	0.211

1187

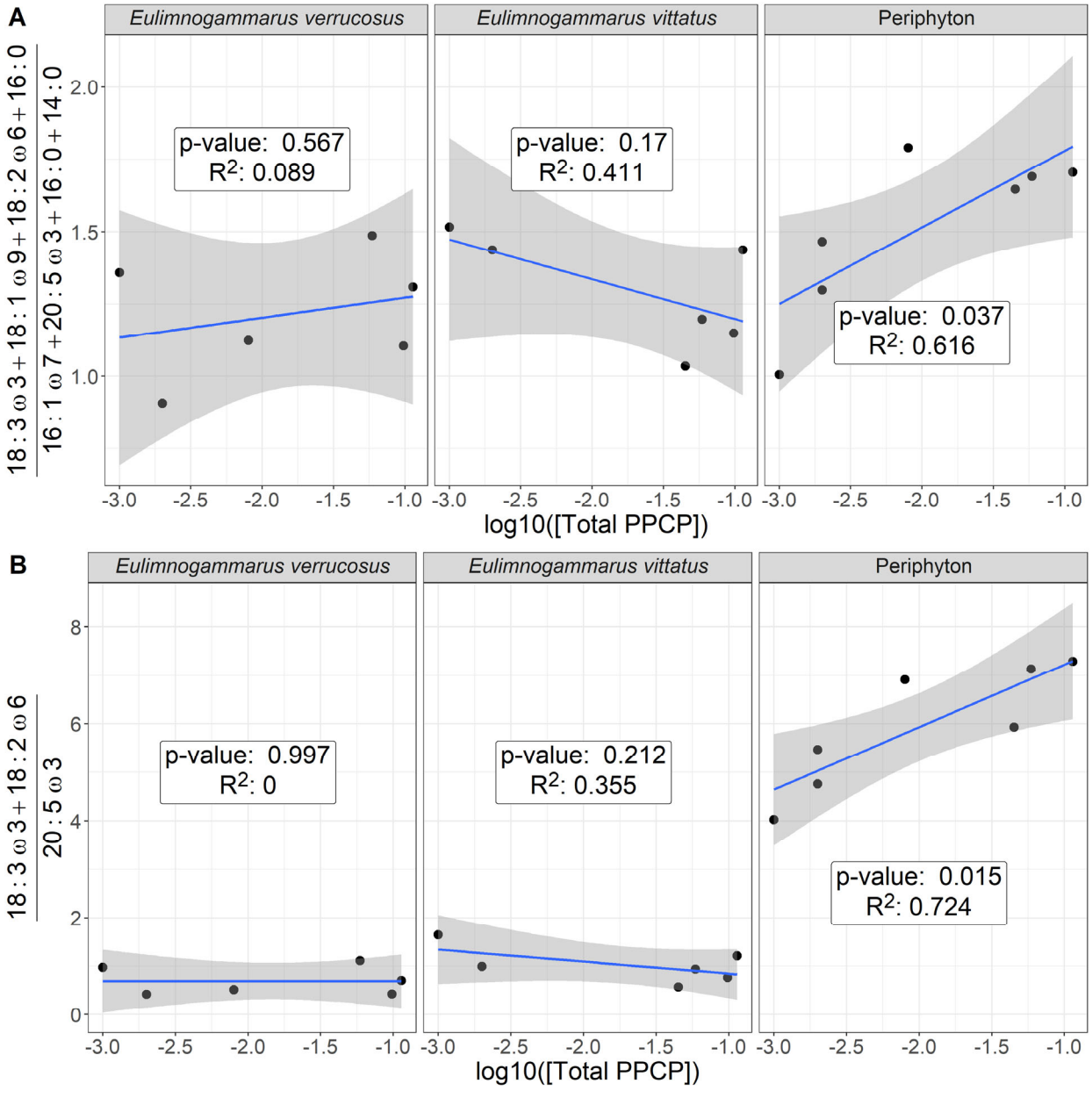

Figure 7: Ratio of filamentous:diatom-associated fatty acids (A) and essential fatty acids (B) across our PPCP gradient. Our first analysis (A) focused solely on green filamentous algal fatty acids (i.e., 18:3ω3, 18:1ω9, 18:2ω6, and 16:0 relative to diatom fatty acids (i.e., 20:5ω3, 16:1ω7, 16:0, 14:0) in relation to increasing PPCP concentrations. This first analysis suggested periphyton reflected an increasing green, filamentous signature relative to diatoms, which

corroborates analyses showing community compositional shifts (Figure 4). While periphyton fatty acids changed significantly across our sewage gradient, macroinvertebrate signatures remained consistent. Our second analysis (B) focused solely on the essential fatty acids, which further highlights the trends observed in periphyton and macroinvertebrate grazers.

Table S1: Macroinvertebrate taxonomic groupings for abundance estimates. Amphipod taxa were defined as in Takhteev & Didorenko, 2015; mollusk taxa were defined as in Sitnikova, 2012.

Amphipoda	**Mollusca**	**Other**
Brandtia latissima intermida (Dorogostaiskii 1930)	Acroloxidae	Asellidae
Brandtia latissima lata (Dybowsky 1874)	Baicaliidae	Caddisflies
Brandtia latissima latior (Dybowsky 1874)	Benedictidate	Hirudinea
Brandtia latissima latissima (Gerstfeldt 1858)	Maackia	Planaria
Brandtia parasitica parasitica (Dybowsky 1874)	Planorbidae	
Cryptoropus inflatus (Dybowsky 1874)	Valvatidae	
Cryptoropus pachytus (Dybowsky 1874)		
Cryptoropus rugosus (Dybowsky 1874)		
Eulimnogammarus capreolus (Dybowsky 1874)		
Eulimnogammarus cruentes (Dorogostaiskii 1930)		
Eulimnogammarus cyaneus (Dybowsky 1874)		
Eulimnogammarus grandimanus (Bazikalova 1945)		
Eulimnogammarus maacki (Gerstfeldt 1858)		
Eulimnogammarus marituji (Bazikalova 1945)		
Eulimnogammarus verucossus (Gerstfeldt 1858)		
Eulimnogammarus viridis viridis (Dybowsky 1874)		
Eulimnogammarus vittatus (Dybowsky 1874)		
Pallasea brandtia brandita (Dybowsky 1874)		
Pallasea brandtii tenera (Sovinskii 1930)		

Pallasea cancelloides (Gerstfeldt 1858)		
Pallasea cancellus (Pallas 1776)		
Pallasea viridis (Garjajev 1901)		
Poekilogammarus crassimus (Sovinskii 1915)		
Poekilogammarus ephippiatus (Dybowsky 1874)		
Poekilogammarus megonychus perpolitus (Takhteev 2002)		
Poekilogammarus pictus (Dybowsky 1874)		

1199

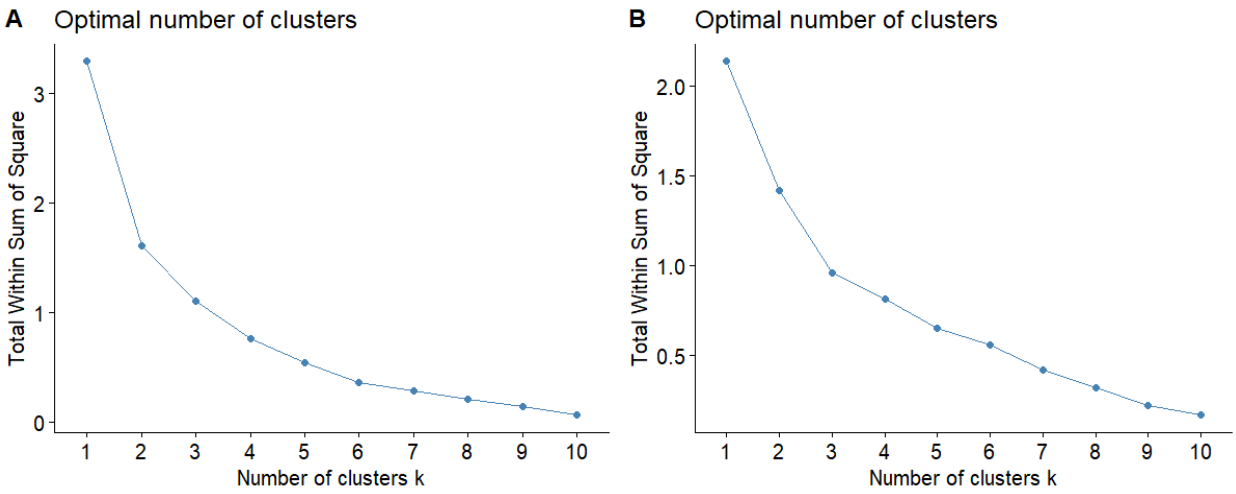

Figure S1: With-group-sum-of-squares (wss) for increasing number of k-mediod clusters for periphyton (A) and invertebrate (B) community data. In the case of periphyton data, wss decreases most markedly with three clusters, whereas invertebrate community abundance is best described by potential two or three clusters.

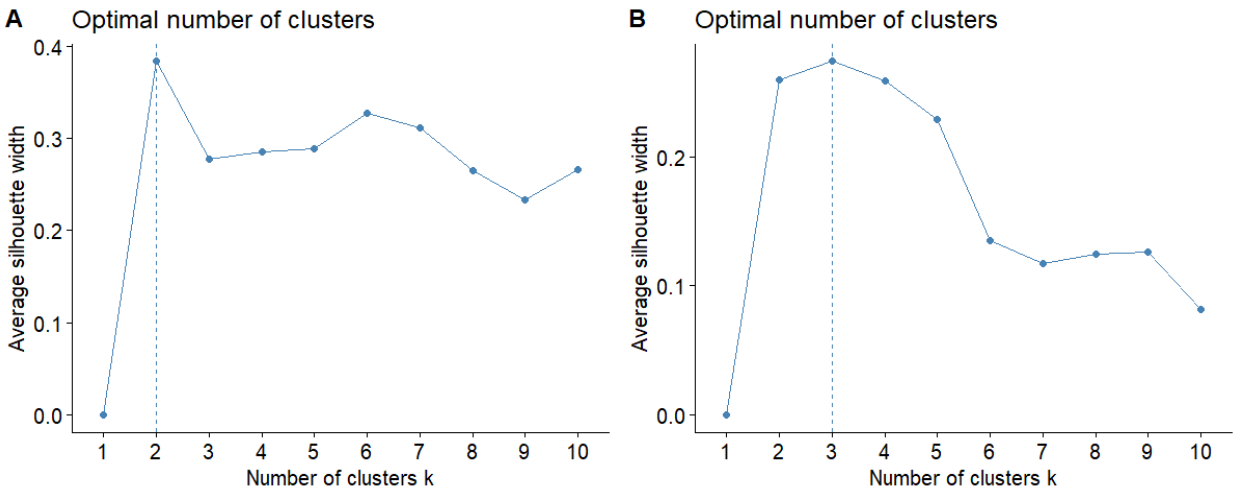

Figure S2: Average silhouette width for increasing number of k-mediod clusters for periphyton (A) and invertebrate (B) community data. In the case of periphyton data, average silhouette width decreases most markedly with three clusters, whereas invertebrate community abundance is best described by two or three clusters as the average silhouette width for both two and three clusters was highest before beginning to decrease.

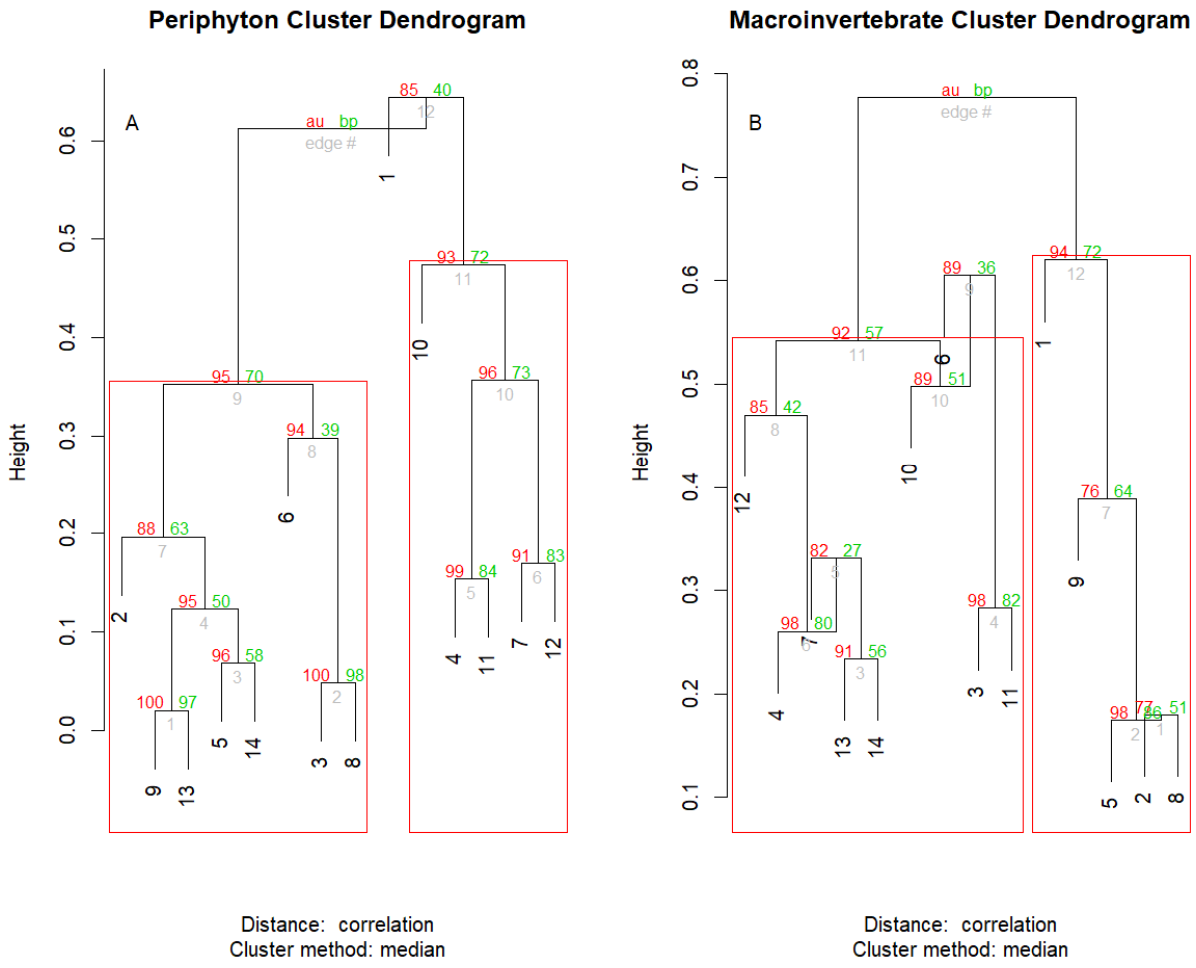

Figure S3: Weighted Pair-Group Centroid Clustering (WPGMC) for periphyton (A) and macroinvertebrate (B) community compositions. Approximately unbiased (au) p-values are computed by multiscale bootstrap resampling, and displayed in red on the left side of each node. Bootstrapped probabilities (bp) are displayed in green on the right side of each node. Unlike k-mediods, WPGMC uses a hierarchical approach to assign clusters, which are bootstrapped in order to generated a probability of group membership. This technique suggested that both periphyton and macroinvertebrates could be grouped in two clusters. Grouping macroinvertebrates into three clusters was possible; however, three clusters resulted in 8 of the

14 sampling locations being assigned to a group. In contrast, two groups enabled 13 of the 14 sampling locations to be assigned to a cluster.

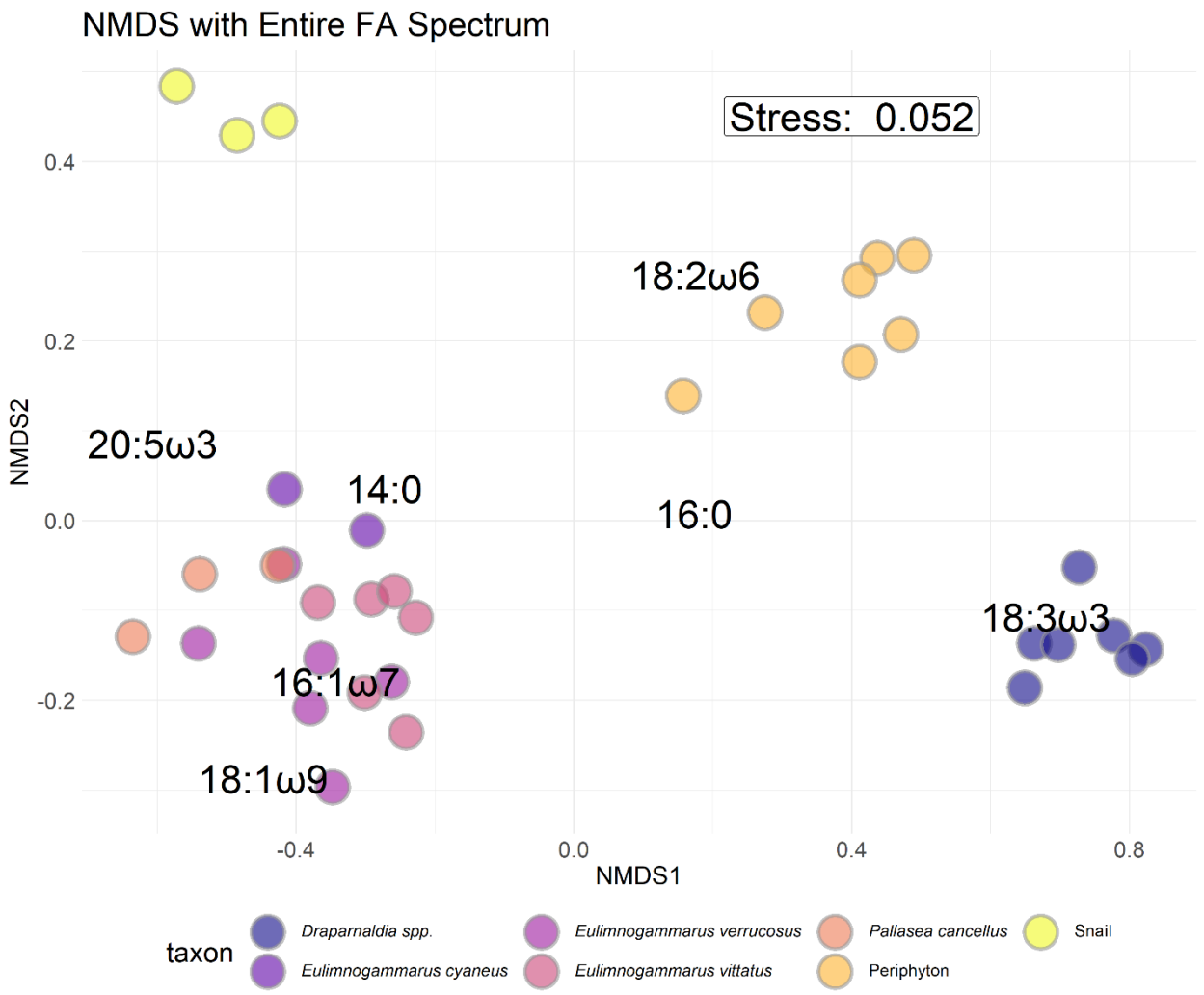

Figure S2: NMDS with Bray-Curtis dissimilarity of proportional fatty acid compositions for each macroinvertebrate and primary producer collected. *Eulimnogammarus* and *Pallasea* are endemic amphipod genera. *Draparnaldia* spp. are endemic filamentous algae that are large and form very dense mats easily collected where it occurs. *Draparnaldia* spp. occurred in large, visible colonies, allowing us to sample and analyze just the *Draparnaldia* spp. fatty acids. Because *Draparnaldia* spp.fatty acids were dominated by 18:3ω3 more so than periphyton, they formed their own cluster. Snails were not identified to species prior to fatty acid analysis. Interspecific variation in fatty acid composition tended to be larger than intraspecific variation, implying that fatty acid signatures were largely species-specific and not environmentally driven.

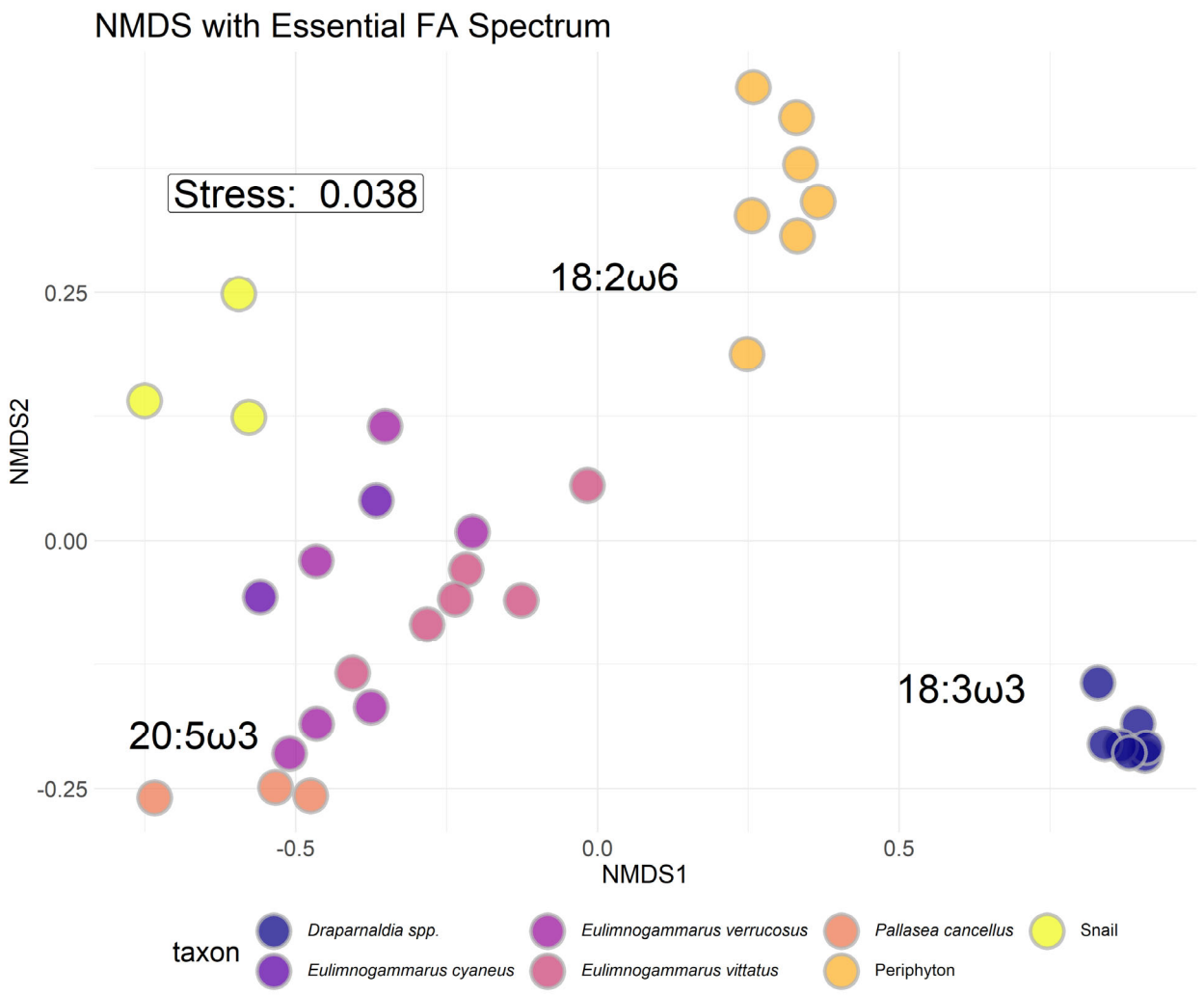

Figure S3: NMDS with Bray-Curtis dissimilarity of proportional biologically essential fatty acid compositions for each macroinvertebrate and primary producer collected. *Eulimnogammarus* and *Pallasea* are endemic amphipod genera. *Draparnaldia* spp. are endemic filamentous algae that are large and form very dense mats easily collected where it occurs. *Draparnaldia* spp. occurred in large, visible colonies, allowing us to sample and analyze just the *Draparnaldia* spp. fatty acids. Because *Draparnaldia* spp. fatty acids were dominated by 18:3ω3 more so than periphyton, they formed their own cluster. Snails were not identified to species prior to fatty acid analysis. Interspecific variation in fatty acid composition tended to be larger than intraspecific

variation, implying that fatty acid signatures were largely species-specific and not environmentally driven.

Table S2: Fatty acid groupings used in this analysis	
Fatty Acid Group	Fatty acids considered
Branched	a-15:0, i-15:0, a-17:0, i-17:0
SAFA	12:0, 14:0, 15:0, 16:0, 17:0, 18:0, 20:0, 22:0, 24:0
MUFA	14:1ω5, 15:1ω7, 17:1n7, 16:1ω5, 16:1ω6, 16:1ω7, 16:1ω8, 16:1ω9, 18:1ω7, 18:1ω9, 20:1ω7, 20:1ω9, 22:1ω7, 22:1ω9
SCPUFA	16:2ω4, 16:2ω6, 16:2ω7, 16:3ω3, 16:3ω4, 16:3ω6, 16:4ω1, 16:4ω3, 18:2ω6, 18:2ω6t, 18:3ω3, 18:3ω6, 18:4ω3, 18:4ω4, 18:5ω3
LCPUFA	20:2ω5(11), 20:2ω5(13), 20:2ω6, 20:3ω3, 20:3ω6, 20:4ω3, 20:4ω6, 20:5ω3, 22:2ω6, 22:3ω3, 22:4ω3, 22:4ω6, 22:5ω3, 22:5ω6, 22:6ω3

1247

1248

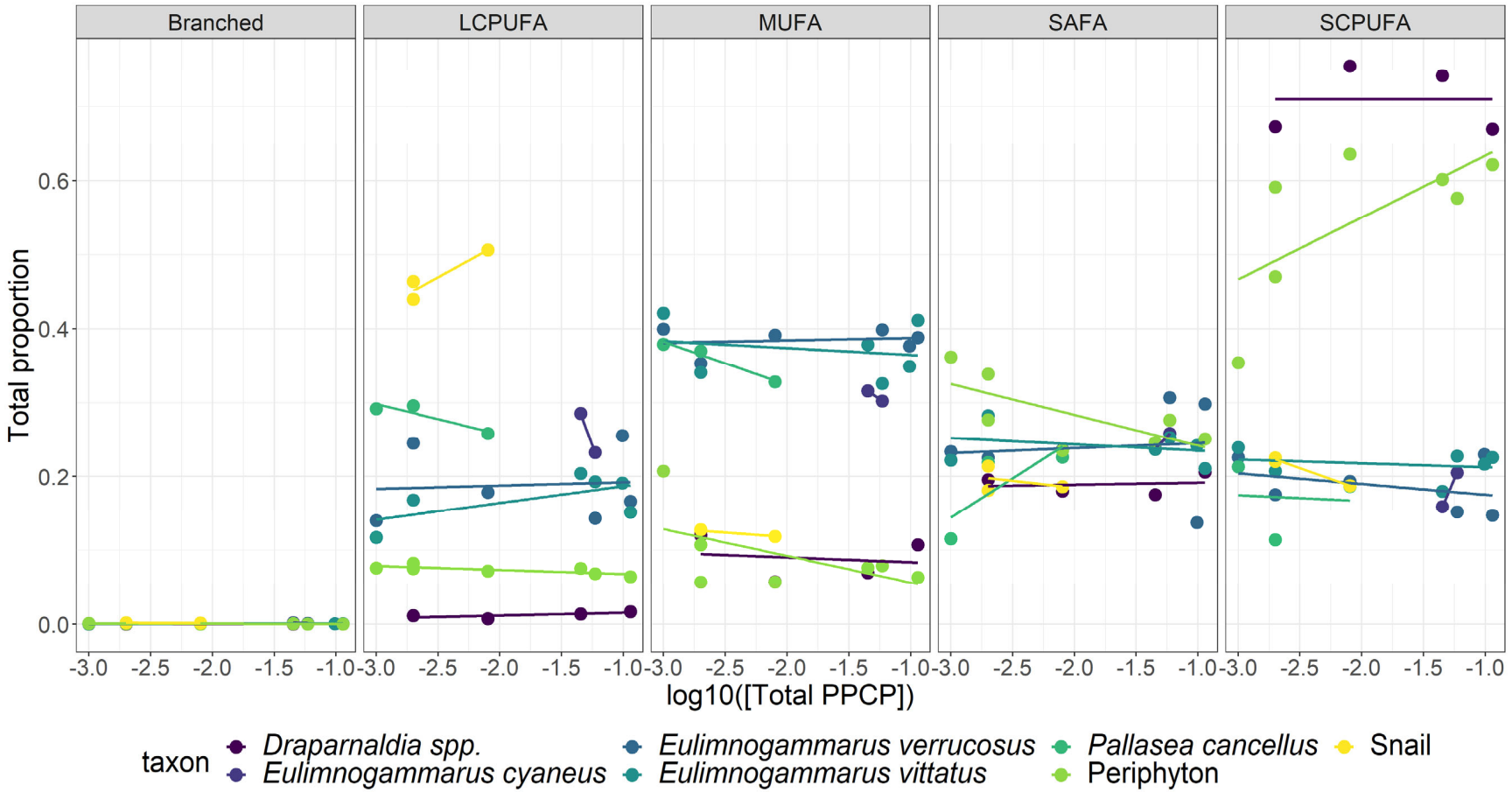

1249

1250 Figure S4: Proportions of major fatty aid groups (as defined in Table S2) across the sewage gradient. Primary producers

1251 (*Draparnaldia* spp. and periphyton) were largely characterized by SCPUFAs, amphipods were largely associated with high MUFA

1252 abundance, and snails were generally characterized with high LCPUFA abundance. Across the sewage gradient, periphyton SCPUFA

1253 tended to increase, which lead to more targeted analyses on which specific fatty acids were increasing. In contrast to periphyton, all
1254 other taxa remained consistent with respect to fatty acid proportions across the sewage gradient.
1255
1256

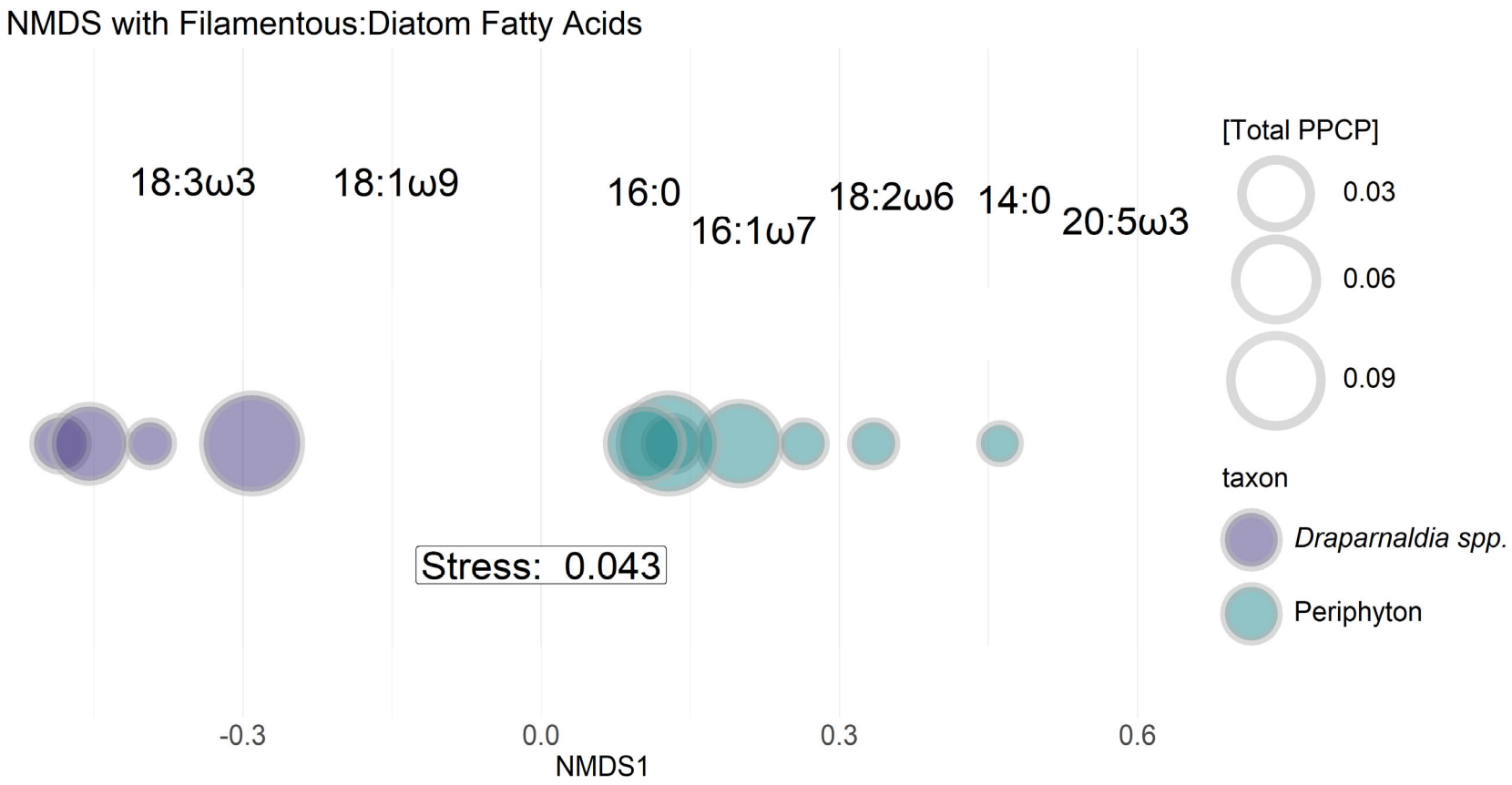

1257

1258 Figure S5: One-dimensional NMDS with Bray-Curtis similarity of seven targeted fatty acids of interest for primary producers. Fatty

1259 acid scores are placed above shapes. Shapes are sized by total PPCP concentration. Periphyton (blue-green) tend to increase in size

1260 from right-to-left, suggesting that periphyton tend to include more 18:3ω3 and 18:1ω9 (indicators of green algal taxa) with an

1261 increasing sewage signal. In contrast, *Draparnaldia* spp. (purple) fatty acids tend to remain consistent across the sewage gradient.

1262

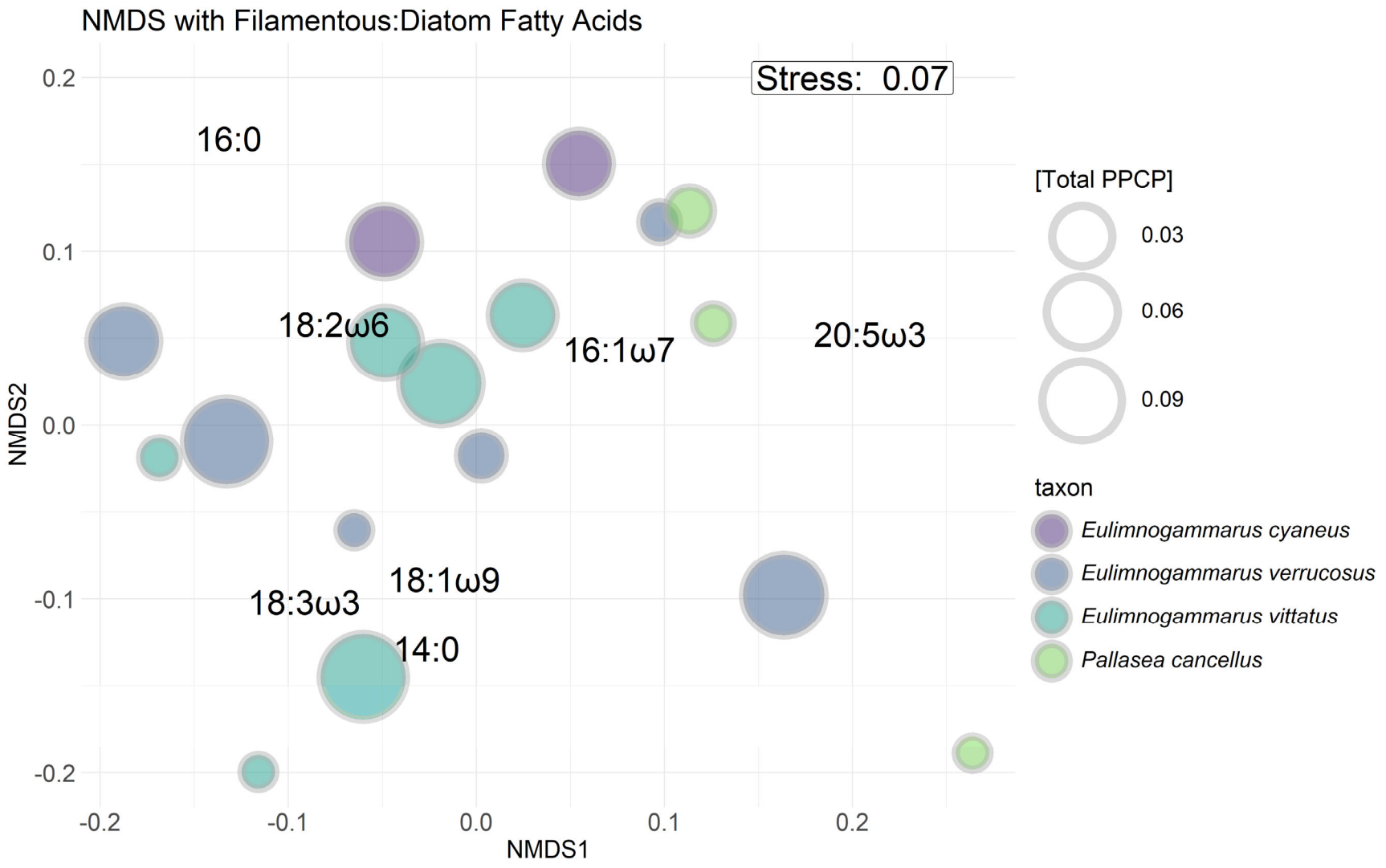
NMDS with Filamentous:Diatom Fatty Acids
Stress: 0.07
16:0
18:2ω6
16:1ω7
20:5ω3
18:1ω9
18:3ω3
14:0
NMDS1
NMDS2
0.2
0.1
0.0
-0.1
-0.2
[Total PPCP]
0.03
0.06
0.09
taxon
Eulimnogammarus cyaneus
Eulimnogammarus verrucosus
Eulimnogammarus vittatus
Pallasea cancellus

1263

Figure S6: NMDS with Bray-Curtis similarity of seven targeted fatty acids of interest for primary producers. Points are sized by total PPCP concentration. Visually, there appears to be no distinct separation among or within taxa unlike was observed with periphyton (Figure S5).

1267